Atmos. Chem. Phys. Discuss., doi:10.5194/acp-2017-456, 2017
Manuscript under review for journal Atmos. Chem. Phys.
Discussion started: 29 May 2017

Atmospheric Chemistry and Physics Discussions

The Role of Meteorological Conditions and Pollution Control Strategies in Reducing Air Pollution in Beijing during APEC 2014 and Parade 2015

Pengfei Liang[1], Tong Zhu[1*], Yanhua Fang[1], Yingruo Li[1, 2], Yiqun Han[1], Yusheng Wu[1], Min Hu[1], and Junxia Wang[1]

[1]SKL-ESPC and BIC-ESAT, College of Environmental Sciences and Engineering, Peking University, Beijing, 100871, China

[2]Environmental Meteorology Forecast Center of Beijing-Tianjin-Hebei, China Meteorological Administration, Beijing, 100089, China

[*]Correspondence to: Tong Zhu (tzhu@pku.edu.cn)

Abstract

To control severe air pollution in China, comprehensive pollution control strategies have been implemented throughout the country in recent years. To evaluate the effectiveness of these strategies, the influence of meteorological conditions on levels of air pollution needs to be determined. We therefore developed a generalized linear regression model (GLM) to establish the relationship between the concentrations of air pollutants and meteorological parameters. Using the intensive air pollution control strategies implemented during the Asia-Pacific Economic Cooperation Forum in 2014 (APEC 2014) and the Victory Parade for the Commemoration of the 70th

Atmos. Chem. Phys. Discuss., doi:10.5194/acp-2017-456, 2017
Manuscript under review for journal Atmos. Chem. Phys.
Discussion started: 29 May 2017

Atmospheric Chemistry and Physics Discussions

Anniversary of the Chinese Anti-Japanese War and the World Anti-Fascist War in 2015 (Parade 2015) as examples, we estimated the role of meteorological conditions and pollution control strategies in reducing air pollution levels in Beijing. During the APEC (1 October to 31 December 2014) and Parade (1 August to 31 December 2015) sampling periods, atmospheric particulate matter of aerodynamic diameter ≤ 2.5 μm ($PM_{2.5}$) samples were collected and gaseous pollutants (SO_2, NO, NO_x, and O_3) were measured online at a site in Peking University (PKU). The concentrations of all pollutants except ozone decreased dramatically (by more than 20%) during both events, compared with the levels during non-control periods. To determine the influence of meteorological conditions on the levels of air pollution, we first compared the air pollutant concentrations during days with stable meteorological conditions (i.e. when the daily average wind speed (WS) was less than 2.50 m s^{-1} and planetary boundary layer (PBL) height was lower than 290 m). We found that the average $PM_{2.5}$ concentration during APEC decreased by 45.7% compared with the period before APEC and by 44.4% compared with the period after APEC. This difference was attributed to emission reduction efforts during APEC. However, there were few days with stable meteorological conditions during Parade. As such, we were unable to estimate the level of emission reduction efforts during this period. Finally, GLMs based only on meteorological parameters were built to predict air pollutant concentrations, which could explain more than 70% of the variation in air pollutant concentration levels, after incorporating the nonlinear relationships between certain meteorological parameters and the concentrations of air pollutants. Evaluation of the GLM

Atmos. Chem. Phys. Discuss., doi:10.5194/acp-2017-456, 2017
Manuscript under review for journal Atmos. Chem. Phys.
Discussion started: 29 May 2017

performance revealed that the GLM, even based only on meteorological parameters, could be satisfactory to estimate the contribution of meteorological conditions in reducing air pollution, and hence the contribution of control strategies in reducing air pollution. Using the GLM, we found that the meteorological conditions and pollution control strategies contributed 30% and 28% to the reduction of the $PM_{2.5}$ concentration during APEC 2014, and 38% and 25% during Parade 2015. We also estimated the contribution of meteorological conditions and control strategies implemented during the two events in reducing the concentrations of gaseous pollutants and $PM_{2.5}$ components with the GLMs, revealing the effective control of anthropogenic emissions.

1 Introduction

Air pollution poses serious health risks to human populations and is one of the most important global environmental problems. To control air pollution in China, the State Council of China (2013) has released the Action Plan for Air Pollution Prevention and Control, which sets pollution control targets for different regions, e.g. atmospheric particulate matter of aerodynamic diameter $\leq$ 2.5 μm ($PM_{2.5}$) concentrations in 2017 shall fall in Beijing–Tianjin–Hebei (BTH) by 25%, in the Yangtze River Delta by 20%, and in the Pearl River Delta by 15%, compared with 2012 levels. To meet these targets, comprehensive pollution control strategies have been implemented at the national, provincial, and city levels. However, it is not clear how effective these strategies are in reducing air pollution. One of the challenges in evaluating the effectiveness of these strategies is that the long-term strategies cannot improve air quality in the short term.

Atmos. Chem. Phys. Discuss., doi:10.5194/acp-2017-456, 2017
Manuscript under review for journal Atmos. Chem. Phys.
Discussion started: 29 May 2017

The efforts made to ensure satisfactory air quality for special events, such as the Beijing 2008 Olympics, provide a unique opportunity to evaluate the effectiveness of pollution control strategies (Kelly and Zhu, 2016). During the Beijing Olympics comprehensive pollution control strategies were implemented intensively over a short period of time. Based on the successful experience during this event, the Chinese government implemented similar air pollution control measures for the 41st Shanghai World Expo in 2010 (SEPB, 2010), the 16th Guangzhou Asian Games and Asian Para Games in 2010 (GEPB, 2009), and the Chengdu Fortune Forum 2013 (CEPB, 2013). To ensure satisfactory air quality in Beijing during the two most recent events: the Asia-Pacific Economic Cooperation Forum in 2014 (APEC 2014) and the Victory Parade for the Commemoration of the 70th Anniversary of the Chinese Anti-Japanese War and the World Anti-Fascist War in 2015 (Parade 2015), the Chinese central government and the local government in Beijing, together with its surrounding provinces, implemented comprehensive air pollution control strategies, including the control of emissions from traffic, industry, and coal combustion, as well as dust pollution control (Table 1). These two events provide a good opportunity to evaluate the effectiveness of air pollution control strategies.

One challenge when evaluating the effectiveness of air pollution control strategies over a short period of time is separating out the contribution of meteorological conditions from the reduction in air pollution levels.

Most previous studies have only provided a descriptive analysis of the changing concentrations of air pollutants during these events. Wen et al. (2016) reported that the

Atmos. Chem. Phys. Discuss., doi:10.5194/acp-2017-456, 2017
Manuscript under review for journal Atmos. Chem. Phys.
Discussion started: 29 May 2017

Atmospheric Chemistry and Physics Discussions

86 average $PM_{2.5}$ concentration during APEC decreased by 54%, 26%, and 39% compared
87 with the levels before APEC in Beijing, Shijiazhuang, and Tangshan, respectively. The
88 authors also reported that the average concentration of total elements in $PM_{2.5}$ during
89 APEC decreased by 75%, 35%, and 36% compared with the levels before APEC in
90 these three sites, respectively. Han et al. (2015) observed that the extinction coefficient
91 and absorbance coefficient decreased significantly during APEC compared with the
92 values before.

93 An increasing number of studies have recognized the importance of
94 meteorological conditions in determining air pollution in Beijing and North China Plain
95 (e.g., Zhang et al., 2012). A northerly wind is considered to be favourable for pollutant
96 diffusion, while a southerly wind is considered to be favourable for the transport of
97 pollutants to Beijing (Zhang et al., 2014). When assessing the effectiveness of air
98 pollution control strategies, a few studies have distinguished between the contribution
99 of meteorological conditions and pollution control strategies in reducing air pollution
100 by comparing air pollutant concentrations under similar meteorological conditions
101 (Wang et al., 2015; Zhang et al., 2009). However, in these studies, days with stable
102 meteorological conditions were determined subjectively, which may introduce
103 uncertainties and inconsistencies when estimating changes in air pollutant
104 concentrations.

105 Statistical models have been developed to establish the relationship between air
106 pollutant concentrations and meteorological parameters. Table 2 summarizes these
107 models, with their respective R^2 values. Multiple linear regression models have been

Atmos. Chem. Phys. Discuss., doi:10.5194/acp-2017-456, 2017
Manuscript under review for journal Atmos. Chem. Phys.
Discussion started: 29 May 2017

widely applied to demonstrate the quantitative relationship between air pollutant concentrations and meteorological parameters, by assuming a linear relationship. However, these relationships are often non-linear (Liu et al., 2007; Liu et al., 2012).

Table 2 shows that most of the models with good explanation ($R^2 > 0.6$) have actually adopted visibility, aerosol optical depth (AOD), and air quality index (AQI) as independent variables to improve the performance of the regression models (Liu et al., 2007; Sotoudeheian and Arhami, 2014; Tian and Chen, 2010; You et al., 2015). This could cause problems in the prediction of air pollutant concentrations during intensive emission control periods because visibility, AOD, and AQI are also dependent on air pollution levels; hence, the statistical models may not function when air pollutant levels are drastically reduced over a short period. A statistical model based solely on meteorological parameters to predict air pollutant concentrations is therefore required.

In this study, we used the air pollution control periods during APEC 2014 and Parade 2015 to estimate the role of meteorological conditions and pollution control strategies in reducing air pollution in the megacity of Beijing. We first measured the changes in air pollutant concentrations, including $PM_{2.5}$, gaseous pollutants, and the components of $PM_{2.5}$. We then estimated the role of meteorological conditions and pollution control strategies in reducing air pollution by comparing the pollutant concentrations during days with stable meteorological conditions. Finally, we developed a statistical model based only on meteorological parameters to evaluate the role of meteorological conditions and pollution control strategies in reducing the levels of air pollution in Beijing. Compared with the models used in previous studies, our

Atmos. Chem. Phys. Discuss., doi:10.5194/acp-2017-456, 2017
Manuscript under review for journal Atmos. Chem. Phys.
Discussion started: 29 May 2017

statistical model had the following advantages: (1) all of the independent variables were meteorological parameters; (2) we considered the non-linear relationships between air pollutant concentrations and meteorological parameters; and (3) in addition to predicting $PM_{2.5}$ mass concentrations, our model could also predict concentrations of gaseous pollutants and individual $PM_{2.5}$ components.

2 Measurements and Methods

2.1 Measurements of Air Pollutants

Gaseous pollutants (SO_2, NO, NO_x, and O_3) were measured online, and $PM_{2.5}$ samples were collected on filters at an urban monitoring station in the campus of Peking University (39.99°N, 116.33°E) northwest of Beijing (Huang et al., 2010). The station is located on the roof of a six-floor building, about 20 m above the ground and about 550 m north of the fourth ring road.

A $PM_{2.5}$ four-channel sampler (TH-16A, Wuhan Tianhong Instruments Co., Ltd., Hubei, China) was used to collect $PM_{2.5}$ samples. The sampling duration was 23.5 h (from 09:30 to 09:00 LT the next day). Both 47-mm quartz filters (QM/A, Whatman, Maidstone, England) and Teflon filters (PTFE, Whatman) were used. The flow rate was calibrated to 16.7 L min^{-1} each week and a blank $PM_{2.5}$ sample was collected once a month. The quartz filters were baked at 550°C for 5.5 h before use. Immediately after collection, the filter samples were stored at −25°C until analysis. A total of 225 $PM_{2.5}$ filter samples were collected during APEC (1 October to 31 December 2014) and Parade (1 August to 31 December 2015) sampling periods. During the sampling periods,

Atmos. Chem. Phys. Discuss., doi:10.5194/acp-2017-456, 2017
Manuscript under review for journal Atmos. Chem. Phys.
Discussion started: 29 May 2017

20 days of $PM_{2.5}$ samples were missed due to rain or sampler failures. Sulphur dioxide (SO_2) was measured with an SO_2 analyzer (43i TL, Thermo Fisher Scientific, Waltham, MA, USA), with a precision of 0.05 ppb. Nitric oxide (NO) and nitrogen oxides (NO_x) were measured with a NO-NO_x analyzer (42i TL, Thermo Fisher Scientific), with precisions of 0.05 ppb for NO and 0.17 ppb for NO_2. Ozone (O_3) was measured with an O_3 analyzer (49i, Thermo Fisher Scientific), with a precision of 1.0 ppb. The SO_2 and NO-NO_x analyzers both had a detection limit of 0.05 ppb, and the O_3 analyzer had a detection limit of 0.50 ppb. All of the gaseous pollutant analyzers had a time resolution of 1 min, and were maintained and calibrated weekly following the manufacturer's protocols.

2.2 Meteorological Data

Meteorological data were obtained from the National Climate Data Center (www.ncdc.noaa.gov) dataset. The meteorological parameters were monitored at a station located in the Beijing Capital International Airport, and consisted of temperature (T), relative humidity (RH), wind direction (WD), wind speed (WS), sea level pressure (SLP), and precipitation (PREC). The PBL height was computed from the simulation results of the National Center for Environmental Prediction (NCEP) Global Data Assimilation System (GDAS) model (www.ready.arl.noaa.gov/READYamet.php).

2.3 Analysis of the $PM_{2.5}$ Filter Samples

To obtain daily average $PM_{2.5}$ mass concentrations, Teflon filters were weighed before and after sampling using an electronic balance, with a detection limit of 10 μg

Atmos. Chem. Phys. Discuss., doi:10.5194/acp-2017-456, 2017
Manuscript under review for journal Atmos. Chem. Phys.
Discussion started: 29 May 2017

(AX105DR) in a super-clean lab (T: 20 ± 1°C, RH: 40 ± 3%). A portion of each Teflon filter was extracted with ultrapure water for the measurement of water-soluble ions (Na^+, NH_4^+, K^+, Mg^{2+}, Ca^{2+}, SO_4^{2-}, NO_3^-, and Cl^-), with an ion-chromatograph (IC-2000 & 2500, Dionex, Sunnyvale, CA, USA). The detection limits of Na^+, NH_4^+, K^+, Mg^{2+}, Ca^{2+}, SO_4^{2-}, NO_3^-, and Cl^- were 0.03, 0.06, 0.10, 0.10, 0.05, 0.01, 0.01, and 0.03 mg L^{-1}, respectively. A portion of each Teflon filter was digested with a solution consisting of nitric acid (HNO_3), hydrochloric acid (HCl), and hydrofluoric acid (HF) for the measurement of trace elements (Na, Mg, Al, Ca, Mn, Fe, Co, Cu, Zn, Se, Mo, Cd, Ba, Tl, Pb, Th and U), with inductively coupled plasma-mass spectrometry (ICP-MS, Thermo X series, Thermo Fisher Scientific). The recoveries for all measured elements fell within ±20% of the certified values. A semi-continuous organic carbon/elemental carbon (OCEC) analyzer (Model 4, Sunset Laboratory, Tigard, OR, USA) was used to analyze organic and elemental carbon from a round punch (diameter: 17 mm) from each quartz filter sample. The T protocol of the National Institute for Occupational Safety and Health (NIOSH) thermal-optical method was applied (see details in Table S1).

All analytical instruments were calibrated before each series of measurements. The R^2 values of the calibration curves for ions, elements, and sucrose concentrations were higher than 0.999.

2.4 Generalized Linear Regression Model (GLM)

A generalized linear regression model (GLM) was used to establish the relationship between air pollutant concentrations and meteorological parameters. The

Atmos. Chem. Phys. Discuss., doi:10.5194/acp-2017-456, 2017
Manuscript under review for journal Atmos. Chem. Phys.
Discussion started: 29 May 2017

objective dependent variables included concentrations of $PM_{2.5}$, individual $PM_{2.5}$ components, and gaseous pollutants.

To match the 23.5-h (09:30–09:00 LT the next day) sampling time of the $PM_{2.5}$ filter samples, metrological parameters were averaged over the same time span (Table 3) and used in the GLM alongside other parameters, e.g. the daily maximum of certain meteorological parameters. The meteorological parameters used in the GLM were T, RH, WD, WS, PBL height, SLP, and PREC. WDs were grouped into three categories, with relevant values and assigned to each category: north (NW, W and NE) as 1, south (SW, SE and E) as 2, and "calm and variable" as 3. A calm wind was defined as when the WS was less than 0.5 m s^{-1}. A variable WD was defined as a condition when: (1) the WD fluctuated by 60° or more during a 2-min evaluation period, with a WS greater than 6 knots (11 km h^{-1}); or (2) the WD was variable and the WS was less than 6 knots (11 km h^{-1}).

A preliminary analysis showed that the concentrations of air pollutants and meteorological parameters fitted best with an exponential function or power function (Figure S2); therefore, these functions were natural log transformed and introduced into the GLM.

We applied the stepwise method to evaluate the level of multicollinearity between the independent variables based on relevant judgement indexes, such as the variance inflation factor (VIF) or tolerance. Based on the assumption that the regression residuals followed a normal distribution and homoscedasticity, which is discussed in a later section, we developed the following model to calculate the concentrations of air

Atmos. Chem. Phys. Discuss., doi:10.5194/acp-2017-456, 2017
Manuscript under review for journal Atmos. Chem. Phys.
Discussion started: 29 May 2017

Atmospheric Chemistry and Physics Discussions

pollutants and chemical components of $PM_{2.5}$ based on meteorological parameters:

$$\ln C_{ij} = \beta_0 + \sum_{k=1}^{m} \beta_{1k} x_k + \sum_{k=1}^{n} \beta_{2k} \ln x_k + \sum_{k=1}^{m'} \beta_{3k} x_k(lag) + \sum_{k=1}^{n'} \beta_{4k} \ln x_k(lag) \quad (1)$$

where C_{ij} is the concentration of the j^{th} air pollutant averaged over the i^{th} day, x_k is the k^{th} meteorological parameter, β_k is the regression coefficient of the k^{th} meteorological parameter, and β_0 is the intercept. For meteorological parameters containing both positive and negative values (i.e. T), only the exponential form was applied. *m*, *n*, *m'*, and *n'* are the number of different forms of meteorological parameters that were eventually included in the model, and were determined based on the stepwise entering method of the regression model. The suffix of *(lag)* refers to the meteorological parameters of the previous day. The main assumption for equation (1) was that the concentrations of air pollutants were only a function of the meteorological parameters, and the emission intensities were constant. Hence, we only used the data before and after APEC 2014 and Parade 2015 control periods in equation (1), excluding the data collected during each period and during the heating season, e.g. after 15 November 2014.

3 Results and Discussion

3.1 Changes of Air Pollutant Concentrations during the APEC 2014 and Parade 2015 Campaigns

Figure 1 shows the time series of $PM_{2.5}$ and the concentrations of its components, as well as the meteorological parameters during the APEC 2014 and Parade 2015 campaigns. The APEC 2014 campaign consisted of three distinct periods: before APEC

Atmos. Chem. Phys. Discuss., doi:10.5194/acp-2017-456, 2017
Manuscript under review for journal Atmos. Chem. Phys.
Discussion started: 29 May 2017

Atmospheric Chemistry and Physics Discussions

(BAPEC, 18 October to 2 November 2014), during APEC (APEC, 3 to 12 November 2014), and after APEC (AAPEC, 13 to 22 November 2014). The Parade 2015 campaign was also divided into three distinct periods: before Parade (BParade, 1 to 19 August 2015), during Parade (Parade, 20 August to 3 September 2015), and after Parade (AParade, 4 to 23 September 2015).

There were two pollution episodes during APEC, on 4 November and 7–10 November 2014, which corresponded to two relatively stable periods with low WS, mainly from the south. The T declined gradually from 12.2°C before APEC to 4.9°C after APEC, and the RH was above 60% during the two pollution episodes. During Parade, the $PM_{2.5}$ concentrations were low during the whole control period, with the prevailing WD from the north and low WS. The T was mostly higher than 20°C, which differed from that during the APEC campaign when it was lower than 20°C.

Table 4 lists the mean concentrations and standard deviations of $PM_{2.5}$, gaseous pollutants, and $PM_{2.5}$ components during the APEC and Parade campaigns. The mean concentration of $PM_{2.5}$ during APEC was 48 ± 35 μg m^{-3}, 58% lower than during BAPEC (113 ± 62 μg m^{-3}), and 51% lower than during AAPEC (97 ± 84 μg m^{-3}). The mean concentration of $PM_{2.5}$ during Parade was 15 ± 6 μg m^{-3}, 63% lower than during BParade (41 ± 14 μg m^{-3}), and 62% lower than during AParade (39 ± 28 μg m^{-3}).

Figure 1 here

Figure 2 shows the proportion of the measured $PM_{2.5}$ components, including OC; EC; the sum of the sulphate, nitrate, and ammonia (SNA); and chloride ion (Cl^-) and trace elements, which together accounted for 70–80% of the total $PM_{2.5}$ mass

Atmos. Chem. Phys. Discuss., doi:10.5194/acp-2017-456, 2017
Manuscript under review for journal Atmos. Chem. Phys.
Discussion started: 29 May 2017

concentration. The proportions of OC (23.5%) and EC (3.5%) in $PM_{2.5}$ were highest during APEC. The proportion of SNA in $PM_{2.5}$ during APEC (40.6%) was lower than during BAPEC (50.7%) and higher than during AAPEC (37.2%). The proportions of Cl^- (4.3%) and elements (6.8%) in $PM_{2.5}$ during APEC were higher than during BAPEC and lower than during AAPEC. For the Parade campaign, the proportions of OC (26.6%) and elements (6.6%) in $PM_{2.5}$ were highest during Parade. The proportions of EC (4.9%) and Cl^- (1.1%) in $PM_{2.5}$ during Parade were higher than during BParade and lower than during AParade. The proportion of SNA in $PM_{2.5}$ was lowest during Parade (37.3%). Similarly, during the pollution control periods of APEC and Parade, the proportions of OC and elements in $PM_{2.5}$ tended to increase and the proportion of SNA in $PM_{2.5}$ tended to decrease.

Figure 2 here

EC is usually considered to be a marker of anthropogenic primary sources, while the sources of OC include both primary and secondary organic aerosols. The correlation between OC and EC can reflect the origin of carbonaceous fractions (Chow et al., 1996). Figure 3 shows the correlation between EC and OC concentrations during the APEC and Parade campaigns. During the APEC and Parade campaigns, the correlation coefficient during both control periods (R^2 = 0.9032) was larger than that during non-control periods (R^2 = 0.6468), indicating that OC and EC were mainly derived from the same sources during both pollution control periods, and were from different sources during the non-control periods. The slope of the OC/EC correlation during the pollution control period was 6.86, which was higher than that during the non-control period (3.97).

Atmos. Chem. Phys. Discuss., doi:10.5194/acp-2017-456, 2017
Manuscript under review for journal Atmos. Chem. Phys.
Discussion started: 29 May 2017

Atmospheric Chemistry and Physics Discussions

This could be due to high levels of secondary OC (SOC) formation during the control periods, and/or the higher contribution from residential solid fuel (coal and biomass) burning (Liu et al., 2016).

Figure 3 here

Figure 4 shows the proportion of SNA in $PM_{2.5}$ ($\rho(SNA)/PM_{2.5}$), the sulphur (S) oxidation ratio (SOR = $[SO_4^{2-}]/([SO_2]+[SO_4^{2-}])$), and nitrogen oxidation ratio (NOR = $[NO_3^-]/([NO_x]+[NO_3^-])$), along with $PM_{2.5}$ concentrations during the APEC (a) and Parade (b) campaigns. During APEC, the average $\rho(SNA)/PM_{2.5}$ was 27%, which was significantly lower than during BAPEC (42%). During Parade, the average $\rho(SNA)/PM_{2.5}$ was 35%, which was also significantly lower than during BParade (47%).

During the APEC campaign, the average SO_2 concentration was 11.3 μg m^{-3} before APEC, 9.5 μg m^{-3} during APEC, and 34.8 μg m^{-3} after APEC, respectively. The average NO_x concentration was 151 μg m^{-3} before APEC, 81 μg m^{-3} during APEC, and 220 μg m^{-3} after APEC, respectively. During the Parade campaign, the average SO_2 concentration during Parade was 1.6 μg m^{-3}, lower than both during BParade (2.7 μg m^{-3}) and AParade (5.9 μg m^{-3}). The average NO_x concentration was also lower during Parade (26 μg m^{-3}), than during BParade (57 μg m^{-3}) and AParade (63 μg m^{-3}).

During the APEC campaign, both the SOR and NOR declined gradually. The average SOR was 42%, 27%, and 17% in the BAPEC, APEC, and AAPEC periods, respectively. The average NOR was 13%, 8%, and 5% in the BAPEC, APEC, and AAPEC periods, respectively. SOR and NOR exhibited different patterns during the Parade campaign. The average SOR was 75%, 64%, and 55% in the BParade, Parade,

Atmos. Chem. Phys. Discuss., doi:10.5194/acp-2017-456, 2017
Manuscript under review for journal Atmos. Chem. Phys.
Discussion started: 29 May 2017

Atmospheric Chemistry and Physics Discussions

and AParade periods, respectively. The average NOR was 8%, 5%, and 8% in the BParade, Parade, and AParade periods, respectively. The SOR was higher during the Parade campaign (64%) than during the APEC campaign (30%). For NOR, a higher average value was found during the APEC campaign (9%) than during the Parade campaign (7%).

The APEC campaign occurred during autumn and early winter, while the Parade campaign occurred during late summer and autumn. The active photochemical oxidation during the Parade campaign resulted in high SO_2-to-sulphate transformation rates, as indicated by the high SOR. In addition, the higher RH in summer favoured the heterogeneous reaction of sulphate formation. For NOR, the T was higher during Parade than during APEC, which favoured the volatilization of nitric acid and ammonia from the particulate phase of nitrate.

These results indicate significant reductions of air pollution during the pollution control periods of APEC 2014 and Parade 2015. However, it is necessary to evaluate if meteorological conditions contributed to this improvement.

Figure 4 here

3.2 Reduction of Air Pollution under Similar Meteorological Conditions

Figure 5 shows the prevalence of WD during the APEC and Parade campaigns. During APEC, the prevailing WD was from the north and northwest, and accounted for 30–40% of the wind frequency. The mean WS during APEC was 3.1 m s^{-1}, higher than during BAPEC (2.2 m s^{-1}) and AAPEC (2.4 m s^{-1}). The “calm and variable” proportion

Atmos. Chem. Phys. Discuss., doi:10.5194/acp-2017-456, 2017
Manuscript under review for journal Atmos. Chem. Phys.
Discussion started: 29 May 2017

of APEC was 28.5%, which was lowest during the APEC campaign. During Parade, a northern and northeastern WD accounted for more than 30% of the wind frequency, and the "calm and variable" proportion was 18.5%, much lower than during BParade and AParade (25.7% and 20.3%, respectively).

Figure 5 here

Figure 6 shows a time series of daily average $PM_{2.5}$ concentrations and PBL heights during the APEC and Parade campaigns, indicating that they have an anti-correlation. In both the BAPEC and AAPEC periods, the PBL heights were mostly less than 400 m. Compared with during APEC and during Parade, the PBL heights were constantly high, which was much more favourable for the diffusion of air pollutants during the control period.

Both WS and PBL height during APEC and Parade were favourable for pollutant diffusion. Therefore, it is necessary to consider meteorological conditions when assessing the impacts of pollution control. One way to do this is to compare air pollution concentrations during periods when meteorological conditions were the same, i.e. under stable conditions (Wang et al., 2015; Zhang et al., 2009).

Figure 6 here

3.2.1 Identify Stable Meteorological Periods

Stable conditions can be defined based on the relationship between air pollution levels and both WSs and PBL height. Figure 7 shows scatter plots between $PM_{2.5}$ concentrations and WS and PBL heights. The relationship can be fitted with a power

Atmos. Chem. Phys. Discuss., doi:10.5194/acp-2017-456, 2017
Manuscript under review for journal Atmos. Chem. Phys.
Discussion started: 29 May 2017

function. A stable condition could be defined by identifying the turning points when the slopes changed from large to relatively small values, and stable conditions could be defined when WSs and PBL heights were lower than the values of the turning points.

The slopes of the power function were monotone, varying with no inflection point. Thus, we used piecewise functions to identify the turning points. As Figure 7 shows, the intersections of two fitting lines represented the turning points of the meteorological influence on $PM_{2.5}$; thus, we defined days with stable meteorological conditions to be those with a daily average WS less than 2.50 m s^{-1} and a daily average PBL height lower than 290 m. We could then compare the corresponding pollutant concentrations between days with stable meteorological conditions.

Figure 7 here

3.2.2 Variation of Air Pollutant Concentrations under Stable Meteorological Conditions

The days with stable meteorological conditions were determined with the method introduced in Section 3.2.1. As a result, eight days before APEC (18, 22, 23, 24, 28, 29, 30, and 31 October 2014), six days during APEC (3, 4, 7, 8, 9, and 10 November 2014), and seven days after APEC (14, 15, 17, 18, 19, 20, and 22 November 2014) were defined as having stable meteorological conditions. Table 5 lists the meteorological conditions (WSs and PBL heights), and the concentrations of pollutants on the days with stable meteorological conditions during the APEC campaign. For the Parade campaign, only one day in each of the BParade, Parade, and AParade periods was defined as having stable meteorological conditions. This was considered to not be well

Atmos. Chem. Phys. Discuss., doi:10.5194/acp-2017-456, 2017
Manuscript under review for journal Atmos. Chem. Phys.
Discussion started: 29 May 2017

representative of the Parade campaign. Thus, we only assessed the variation of air pollutant concentrations during stable meteorological periods of the APEC campaign.

For days with stable meteorological conditions during the APEC campaign, the average WS was 1.4, 1.9, and 1.7 m s^{-1} in the BAPEC, APEC, and AAPEC periods, respectively; and the average PBL height was 191, 194, and 160 m in the same three periods, respectively. This clearly shows that the meteorological conditions of days considered to be stable throughout the APEC campaign were very similar.

Figure 8 shows the percentage reductions calculated by comparing the decreased average concentrations for all days during APEC to the average concentrations before APEC in black bars, and the percentage reductions based on the days with stable meteorological conditions in red bars. For the difference between the APEC and BAPEC periods, the percentage reduction on days with stable meteorological conditions was much lower than the reduction calculated when considering all days, except for Ca and NO. This indicates that the method applied to days with stable meteorological conditions excluded part of the meteorological influence on pollutant concentrations.

The standard deviations were also calculated with an error transfer formula that is described in detail in the Supplementary Information. Figure 8 shows that the standard deviations of the percentage reduction based on days with stable meteorological conditions decreased significantly. For example, the standard deviation of the percentage reduction in $PM_{2.5}$ based on the days with stable meteorological conditions decreased from 39% to 26% compared with the same measurement when all days were

Atmos. Chem. Phys. Discuss., doi:10.5194/acp-2017-456, 2017
Manuscript under review for journal Atmos. Chem. Phys.
Discussion started: 29 May 2017

388 considered. This indicates that by considering only days with stable meteorological
389 conditions, the uncertainties associated with the percentage reduction figures were
390 reduced and the reliability of the changes of air pollutants concentrations were
391 improved.

392 Figure 8 here

393 Figure 9 shows the changes of pollutant concentrations on days with stable
394 meteorological conditions during the APEC campaign. The average $PM_{2.5}$
395 concentration was 70 μg m^{-3} during APEC, which represented a 45.7% decrease
396 compared with the concentration in the BAPEC period (129 μg m^{-3}) and a 44.4%
397 decrease compared with the concentration in the AAPEC period (126 μg m^{-3}).

398 A similar pattern was observed for SNA. The SNA concentration decreased
399 significantly during APEC compared with the BAPEC period. In the BAPEC period,
400 the average sulphate, nitrate, and ammonium concentrations were 13.4, 34.2, and 16.7
401 μg m^{-3}, respectively. During APEC, the average concentrations of sulphate, nitrate and
402 ammonium were 5.6, 17.0, and 7.4 μg m^{-3}, respectively. In the AAPEC period, the
403 average concentrations of sulphate, nitrate, and ammonium were 12.5, 21.8, and 13.6
404 μg m^{-3}, respectively.

405 The average OC concentration was 15.9 μg m^{-3} during APEC, which represented
406 a 15.4% decrease compared with the concentration in the BAPEC period (18.8 μg m^{-3}).
407 In comparison, the average EC concentration was 2.4 μg m^{-3} during APEC, which
408 represented a 35.1% decrease compared with the concentration in the BAPEC period
409 (3.7 μg m^{-3}). This indicates that the reduction of the OC concentration was less

Atmos. Chem. Phys. Discuss., doi:10.5194/acp-2017-456, 2017
Manuscript under review for journal Atmos. Chem. Phys.
Discussion started: 29 May 2017

significant than that of the EC concentration during APEC.

During APEC, the average concentrations of Cl^- and potassium ion (K^+) were 3.1 and 0.96 μg m^{-3}, which represented a decrease of 22.5% and 31.4%, compared with the concentrations in the BAPEC period. The average concentrations of Cl^- and K^+ increased significantly to 8.9 and 2.01 μg m^{-3} in the AAPEC period, which represented an increase of 187.1% and 109.4%, respectively compared with the concentrations during APEC. The average concentrations of several anthropogenic elements, including Pb, Zn, Ni, and Mn, all significantly decreased during APEC compared with the concentrations in the BAPEC and AAPEC periods. In contrast, the average concentration of Ca was 634 ng m^{-3} during APEC, which represented only an 8.2% decrease compared with the concentration before APEC (691 ng m^{-3}), this may be due to the fact that Ca is mainly derived from geogenic sources (Mustaffa et al., 2014; Tao et al., 2014).

The average SO_2 concentration was 12.7 μg m^{-3} during APEC, which was almost equal with that in the BAPEC period (12.9 μg m^{-3}), but it increased significantly to 41.8 μg m^{-3} in the AAPEC period. In comparison, the average concentrations of NO and NO_x decreased significantly during APEC (61.0% and 42.9%, respectively) and increased substantially in the AAPEC period (376.7% and 139.3%, respectively). During APEC, the average concentration of O_3 was 27.1 μg m^{-3}, which represented an increase of 92.2% and 133.6%, compared with the concentrations in the BAPEC and AAPEC periods. The significant increase in the average SO_2 concentration in the AAPEC period was consistent with the increased ratios of the average concentrations

Atmos. Chem. Phys. Discuss., doi:10.5194/acp-2017-456, 2017
Manuscript under review for journal Atmos. Chem. Phys.
Discussion started: 29 May 2017

Atmospheric Chemistry and Physics Discussions

of Cl^- and K^+ in the same period, indicating an increase in coal combustion, which coincided with the government subsidised heating season in north China that started on 15 November. The inverse variation patterns of NO_x and O_3 indicate that the significant increase of O_3 may be because of the decline in average NO_x concentration during the pollution control period of APEC.

Figure 9 here

Table 6 lists the percentage differences among the mean $PM_{2.5}$ concentrations of four periods (P1, P2, P3, and P4) that were randomly selected from within the non-control days of the APEC and Parade campaigns. Based on the assumptions that days with stable meteorological conditions were representative of the corresponding periods during the APEC campaign, and the emission intensities were constant, the percentage differences in the mean $PM_{2.5}$ concentrations between these four random periods should be close to zero. The mean concentrations during P1, P2, P3, and P4 were 120, 101, 96, and 87 μg m^{-3}, respectively. The standard deviation (SD) during P1, P2, P3, and P4 were 97, 58, 40, and 23 μg m^{-3}, respectively, with the average SD being 59 μg m^{-3}. The mean value of the percentage differences of the mean $PM_{2.5}$ concentrations between P1, P2, P3, and P4 was −16%, with a root mean square error (RMSE) of 18%. Hence, uncertainties remain within the percentage differences based on the days with stable meteorological conditions, although the size of these uncertainties was reduced. This may be due to the limited sample size on days with stable meteorological conditions during the APEC campaign. It is therefore necessary to further quantify the meteorological influences.

Atmos. Chem. Phys. Discuss., doi:10.5194/acp-2017-456, 2017
Manuscript under review for journal Atmos. Chem. Phys.
Discussion started: 29 May 2017

Atmospheric Chemistry and Physics Discussions

3.3 Emission Reductions during APEC and Parade Based on GLM Predictions

The previous section showed that the number of days with stable meteorological conditions could be limited; it was therefore impossible to estimate quantitatively the contribution of meteorological conditions to the reduction of air pollutant concentrations. We developed a GLM based only on meteorological parameters to meet this requirement.

3.3.1 Model Performance

Figure 10 shows the scatter plot and correlation between the GLM-predicted and observed concentrations of air pollutants transformed to a natural log. The R^2 values of the linear regression equations ranged from 0.6638 to 0.8542, most of them are higher than 0.7 except for Zn and Mn, indicating that the GLM-predicted concentrations correlated well with the observed concentrations. Specifically, the R^2 value of the linear regression equation for $PM_{2.5}$ is as high as 0.8154.

Figure 10 here

Before applying the GLM to predict the air pollutant concentrations, the cross-validation (CV) method was used to evaluate the performance of the $PM_{2.5}$ model, with the assumption that it was representative of all air pollutants. The data input to the $PM_{2.5}$ model was allocated randomly into five equal periods, namely CV1, CV2, CV3, CV4, and CV5. For each test, one period was removed from the input data and the remaining data were applied to establish the CV model, which was then used to predict the $PM_{2.5}$ concentrations for the removed period. After five rounds, all input data were included

Atmos. Chem. Phys. Discuss., doi:10.5194/acp-2017-456, 2017
Manuscript under review for journal Atmos. Chem. Phys.
Discussion started: 29 May 2017

Atmospheric Chemistry and Physics Discussions

in the CV test. Figure 11 shows the time series of the observed and CV-predicted $PM_{2.5}$ concentrations, which demonstrates a good performance for the $PM_{2.5}$ GLM.

Figure 11 here

Table 7 shows the CV-predicted $PM_{2.5}$ concentrations. The adjusted R^2 values for the five CV periods ranged from 0.710 to 0.807, which was lower than the value (0.808) derived from the $PM_{2.5}$ model, due to the lack of input data. The observed mean $PM_{2.5}$ concentrations were 94, 59, 44, 54, and 41 μg m^{-3} for the five CV periods, respectively. The corresponding CV-predicted mean $PM_{2.5}$ concentrations were 82, 57, 52, 65, and 47 μg m^{-3}, respectively. The relative error (RE) between the observed mean $PM_{2.5}$ concentrations and the CV-predicted mean $PM_{2.5}$ concentrations ranged from −17% to 15%, with a mean RE of −5%. The RMSE of the RE was 14.6%, reflecting the uncertainties of the GLM method in quantitatively estimating the contribution of the meteorological conditions to the air pollutant concentrations.

Table 7 also lists the daily RMSE for each CV period and the total RMSE. The daily RMSE for each CV period was calculated with the daily average $PM_{2.5}$ concentrations during each CV period, and the total RMSE was calculated with the daily average $PM_{2.5}$ concentration throughout all five CV periods combined. The daily RMSE ranged from 19 to 53 μg m^{-3}, and the total RMSE was 33 μg m^{-3}, indicating that the model prediction accuracy at the daily level needs to be improved. Liu et al. (2012) used a generalized additive model (GAM) to predict $PM_{2.5,}$ which had a total daily RMSE of 23 μg m^{-3}. Compared with their results, the CV performance in our study was satisfactory considering that the independent variables in our model were only based

Atmos. Chem. Phys. Discuss., doi:10.5194/acp-2017-456, 2017
Manuscript under review for journal Atmos. Chem. Phys.
Discussion started: 29 May 2017

on meteorological parameters, while the model of Liu et al. (2012) included AOD.

The relative error calculated with the CV method for GLM was −5% (Table 7), which was smaller than the mean percentage difference (−16%) calculated based on days with stable meteorological conditions (Table 6). Moreover, the RMSE of relative error calculated with the CV method for GLM (Table 7) was 14.6%, which was also smaller than the RMSE of percentage difference (18%) calculated based on days with stable meteorological conditions (Table 6).

These indicate that the GLM reduced uncertainties of the method in quantitatively estimating the contribution of the meteorological conditions to the pollutant concentrations.

3.3.2 Residual Analysis of GLM

Table 8 shows the concentrations of air pollutants for the GLM with adjusted R^2 values higher than 0.6. Again, we used the $PM_{2.5}$ model as an example. Table 9 lists the output indexes of the $PM_{2.5}$ GLM, including a model summary, analysis of variance (ANOVA), coefficients, and other indexes. The values of R, R^2, and adjusted R^2 were 0.910, 0.828, and 0.808, respectively, indicating that the $PM_{2.5}$ model can explain 80.8% of the variability of the daily average $PM_{2.5}$ concentrations. The model was statistically significant according to the p-value (<0.05) from an F-test, and the meteorological parameters eventually selected as the independent variables of the model were statistically significant according to the p-values (<0.05) from a t-test. The meteorological parameters eventually included in the model were lnWS, $lnWS_{max(lag)}$,

Atmos. Chem. Phys. Discuss., doi:10.5194/acp-2017-456, 2017
Manuscript under review for journal Atmos. Chem. Phys.
Discussion started: 29 May 2017

Atmospheric Chemistry and Physics Discussions

518 PBL_{max}, PREC, $\ln\Delta T_{(lag)}$, WS_{mode}, $WD/WS_{(lag)}$, $PBL_{min(lag)}$, $PREC_{(lag)}$, and SLP_{min}.
519 According to the collinearity statistics, all the VIF values were within 5 and tolerance
520 values were larger than 0.1, indicating that no serious multicollinearity existed between
521 the independent parameters. The Durbin–Watson value (1.910) was close to 2,
522 accounting for the good independence of the variance.

523 Figure 12 shows a residual analysis of the model. According to the residual
524 histogram (a), the mean value of the regression standardized residual was −0.01, with
525 a standard deviation of 0.955. According to the P-P graph (c), the distribution of the
526 observed and expected cumulative probability spread along the diagonal of $y = x$.
527 According to the de-trended P-P graph (d), the deviations from a normal distribution
528 were within ±0.05. These results indicate that the model residuals followed a normal
529 distribution. The scatter diagram of residuals and simulated values (b) could be applied
530 to test the homoscedasticity, i.e. the distribution of the regression residual did not
531 change over the range of values predicted by the regression. Figure S4 demonstrates
532 the time series of the observed pollutant and GLM-predicted pollutant concentrations,
533 which displayed a good correlation.

534 Figure 12 here

535 **3.3.3 Quantitative Estimates of the Contribution of Meteorological Conditions to**
536 **Air Pollutant Concentrations**

537 We applied the GLM to predict air pollutant concentrations during APEC 2014
538 and Parade 2015 based on meteorological parameters. The difference between the
539 observed and GLM-predicted concentrations was attributed to emission reduction

through the implementation of air pollution control strategies.

Table 10 lists the percentage differences between the observed and GLM-predicted concentrations of air pollutants during APEC and Parade. The mean concentrations of the observed and predicted $PM_{2.5}$ were 48 and 67 μg m^{-3} during APEC, i.e. a 28% difference. The mean concentrations of the observed and predicted $PM_{2.5}$ were 15 and 20 μg m^{-3} during Parade, i.e. a 25% difference. These differences are attributed to the emission reduction through the implementation of air pollution control strategies. As described in Section 3.1, the mean concentrations of $PM_{2.5}$ decreased by 58% and 63% during APEC and Parade, therefore, the meteorological conditions and pollution control strategies contributed 30% and 28% to the reduction of the $PM_{2.5}$ concentration during APEC 2014, respectively, and 38% and 25% during Parade 2015, respectively.

The emission reduction during APEC in this study is comparable to the results of other studies where meteorological influences were considered. For example, the $PM_{2.5}$ concentration decreased by 33% under the same weather conditions during APEC in Beijing as modelled by the Weather Research and Forecasting model and Community Multiscale Air Quality (WRF/CMAQ) model (Wu et al., 2015). In addition, emission control implemented in Beijing during APEC resulted in a 22% reduction in the $PM_{2.5}$ concentration, as modelled by WRF-Chem (Guo et al., 2016).

Same as $PM_{2.5}$, the differences listed in Table 10 for other pollutants show the reduction in emission of these pollutants and/or their precursors. The differences for EC were 37% (from 2.7 to 1.7 μg m^{-3}) during APEC and 33% (from 1.2 to 0.8 μg m^{-3}) during Parade. In contrast, the differences for OC were 11% (from 12.6 to 11.2 μg m^{-3})

Atmos. Chem. Phys. Discuss., doi:10.5194/acp-2017-456, 2017
Manuscript under review for journal Atmos. Chem. Phys.
Discussion started: 29 May 2017

Atmospheric Chemistry and Physics Discussions

562 during APEC and 8% (from 3.7 to 4.0 μg m^{-3}) during Parade. The differences for
563 carbonaceous components (OC + EC) were 16% (from 15.3 to 12.9 μg m^{-3}) during
564 APEC and 2% (from 4.9 to 4.8 μg m^{-3}) during Parade. This indicates that the emission
565 reduction for OC and its precursors were smaller than the reduction of EC during APEC
566 and Parade. A similar pattern was found for the reduction for EC and OC based on days
567 with stable meteorological conditions discussed in Section 3.2.2.

568 Table 10 also shows the differences for sulphate were 44% (from 2.7 to 3.9 μg m^{-3})
569 during APEC and 50% (from 5.2 to 2.6 μg m^{-3}) during Parade. The differences for
570 nitrate were 44% (from 19.0 to 10.6 μg m^{-3}) during APEC and 56% (from 3.4 to 1.5 μg
571 m^{-3}) during Parade. The differences for ammonium were 13% (from 5.5 to 4.8 μg m^{-3})
572 during APEC and 38% (from 2.4 to 1.5 μg m^{-3}) during Parade. In total, the differences
573 for SNA were 29% (from 27.2 to 19.3 μg m^{-3}) during APEC and 49% (from 11.0 to 5.6
574 μg m^{-3}) during Parade.

575 The concentration of sulphate is determined by primary emissions and secondary
576 transformation from SO_2; thus, the changes in sulphate concentrations may not reflect
577 the effectiveness of emission control strategies. One needs to also include the changes
578 in SO_2 concentrations. By adding the molar concentrations of SO_2 and SO_4^{2-} ($S = [SO_2]$
579 + $[SO_4^{2-}]$), the concentration of total S was calculated. Table 10 shows the differences
580 for SO_2 were 50% (from 6.59 to 3.32 ppb) during APEC and 2% (from 0.56 to 0.57
581 ppb) during Parade, while the differences for total S were 41% (from 0.322 to 0.189
582 μmol m^{-3}) during APEC and 33% (from 0.079 to 0.053 μmol m^{-3}) during Parade. Coal
583 combustion emissions is the major contributor to total S, this demonstrates the effective

Atmos. Chem. Phys. Discuss., doi:10.5194/acp-2017-456, 2017
Manuscript under review for journal Atmos. Chem. Phys.
Discussion started: 29 May 2017

584 control of coal combustion during both APEC 2014 and Parade 2015. The difference
585 for SO_2 during APEC was larger than that during Parade, while the difference for
586 sulphate during Parade was larger than that during APEC. As discussed in Section 3.1,
587 the mean SOR was 27% and 64% during APEC and Parade, respectively, indicating
588 that the SO_2-to-sulphate transformation rate during APEC (autumn and early winter)
589 was much lower than during Parade (late summer and autumn).

590 It is interesting to note that the difference for OC during APEC was only 11%
591 (Table 10) and the observed concentration of OC was even 8% higher than the GLM-
592 predicted concentration during Parade, indicating that the control of the OC
593 concentration was not as effective as the control of other $PM_{2.5}$ components during
594 APEC and Parade. This may be because OC can originate from both primary emission
595 and secondary transformation. In contrast, the control of the SNA concentration was
596 very effective during APEC and Parade, leading to a significant decrease of $PM_{2.5}$
597 during both events.

598 Table 10 shows NO_x and other $PM_{2.5}$ components also had significant emission
599 reduction during APEC 2014 and Parade 2015. The differences between the observed
600 and GLM-predicted concentrations of NO_x were 56% (from 102 to 45 ppb) during
601 APEC and 35% (from 20 to 13 ppb) during Parade. The differences for Cl^- were 20%
602 (from 2.58 to 2.06 μg m^{-3}) during APEC and 6% (from 0.17 to 0.16 μg m^{-3}) during
603 Parade. The differences for K^+ were 37% (from 1.03 to 0.65 μg m^{-3}) during APEC and
604 25% (from 0.24 to 0.18 μg m^{-3}) during Parade. The differences for Pb, Zn, and Mn
605 ranged from 21% to 53% during APEC and Parade.

606 The concentrations of Cl^- have been found to be high in the fine particles produced
607 from coal combustion (Takuwa et al., 2006), while the concentrations of K^+ are high in
608 particles derived from combustion activities, e.g. biomass burning and coal combustion.
609 Lead is typically considered to be a marker of emissions from coal combustion, power
610 stations, and metallurgical plants (Dan et al., 2004; Mukai et al., 2001; Schleicher et al.,
611 2011). Zinc can be produced by the action of a car braking and by tire wearing (Cyrys
612 et al., 2003; Sternbeck et al., 2002). Manganese mainly originates from industrial
613 activities. Major sources of NO_x emissions include power plants, industry, and
614 transportation (Liu and Zhu, 2013). The differences for the concentrations of total S,
615 Cl^-, K^+, Pb, Zn, Mn, and NO_x, indicate that the control of anthropogenic emissions,
616 especially coal combustion, was very effective during APEC and Parade.

617 ## 4 Conclusions

618 During the pollution control periods of APEC 2014 and Parade 2015, the
619 concentrations of air pollutants except ozone decreased dramatically compared with the
620 concentrations during non-control periods, accompanied by meteorological conditions
621 favourable for pollutant dispersal.

622 To estimate the contributions of meteorological conditions and pollution control
623 strategies in reducing air pollution, comparing the concentrations of air pollutants
624 during days with stable meteorological conditions is a useful method, but has limitation
625 due to high uncertainty and lack of a sufficient number of days with stable
626 meteorological conditions

627 Our study shows that, if including the nonlinear relationship between
628 meteorological parameters and air pollutant concentrations, GLMs based only on
629 meteorological parameters could provide a good explanation of the variation of
630 pollutant concentrations, with adjusted R^2 values mostly larger than 0.7. Since the
631 GLMs contained no parameters dependent on air pollution levels as independent
632 variables, they could be used to estimate the contributions of meteorological conditions
633 and pollution control strategies to the air pollution levels during emission control
634 periods.

635 With the GLMs method, we found meteorological conditions and pollution control
636 strategies played almost equally important roles in reducing air pollution in megacity
637 Beijing during APEC 2014 and Parade 2015, e.g. 30% and 28% to the reduction of the
638 $PM_{2.5}$ concentration during APEC 2014, as well as 38% and 25% during Parade 2015.
639 We also found that the control of the SNA concentration was more effective than
640 carbonaceous components. The differences between the observed and GLM-predicted
641 concentrations of specific pollutants (Cl^-, K^+, Pb, Zn, Mn, NO_x, and S) related to coal
642 combustion and industrial activities revealed the effective control of anthropogenic
643 emissions.

644 In the future, combining the methods of source apportionment, the contributions
645 of emission reductions for different sources in reducing air pollution could be estimated,
646 enabling further analysis of pollution control strategies.

647

648 **Data availability.** The data of stationary measurements are available upon requests.

649 **Author contribution.** T. Zhu and P. F. Liang designed the experiments. P. F. Liang
650 collected and weighed the $PM_{2.5}$ filter samples. P. F. Liang, Y. H. Fang, Y. Q. Han, and
651 J. X. Wang carried out the analysis of the components in $PM_{2.5}$. Y. S. Wu and M. Hu
652 provided the data of gaseous pollutant concentrations. Y. R. Li computed the data of
653 planetary boundary layer heights from GDAS and P. F. Liang developed the generalized
654 linear regression model. J. X. Wang managed the data. P. F. Liang analyzed the data
655 with contributions from all co-authors. P. F. Liang prepared the manuscript with helps
656 from T. Zhu.

657 **Acknowledgement.** This study was supported by the National Natural Science
658 Foundation Committee of China (41421064, 21190051), the European 7th Framework
659 Programme Project PURGE (265325), and the Collaborative Innovation Center for
660 Regional Environmental Quality.

661 ## Reference

662 Barmpadimos, I., Keller, J., Oderbolz, D., Hueglin, C., and Prevot, A. S. H.: One decade
663 of parallel fine ($PM_{2.5}$) and coarse (PM_{10}-$PM_{2.5}$) particulate matter measurements
664 in Europe: trends and variability, Atmos. Chem. Phys., 12, 3189-3203,
665 doi:10.5194/acp-12-3189-2012, 2012.
666 CEPB: Chengdu Environmental Protection Bureau, available at:
667 http://www.cdepb.gov.cn/cdepbws/Web/Template/GovDefaultInfo.aspx?cid=236
668 &aid=22738 (last assess: 25 May 2017), (in Chinese), 2013.
669 China, S. C. o., State Council of P. R. China's notification on Action Plan for Air
670 Pollution Prevention and Control. 2013.
671 Chitranshi, S., Sharma, S. P., and Dey, S.: Spatio-temporal variations in the estimation
672 of PM_{10} from MODIS-derived aerosol optical depth for the urban areas in the
673 Central Indo-Gangetic Plain, Meteorol. Atmos. Phys., 127, 107-121,
674 doi:10.1007/s00703-014-0347-z, 2015.
675 Chow, J. C., Watson, J. G., Lu, Z. Q., Lowenthal, D. H., Frazier, C. A., Solomon, P. A.,

Thuillier, R. H., and Magliano, K.: Descriptive analysis of $PM_{2.5}$ and PM_{10} at regionally representative locations during SJVAQS/AUSPEX, Atmos. Environ., 30, 2079-2112, doi 10.1016/1352-2310(95)00402-5, 1996.

Chudnovsky, A. A., Koutrakis, P., Kloog, I., Melly, S., Nordio, F., Lyapustin, A., Wang, Y. J., and Schwartz, J.: Fine particulate matter predictions using high resolution Aerosol Optical Depth (AOD) retrievals, Atmos. Environ., 89, 189-198, doi:10.1016/j.atmosenv.2014.02.019, 2014.

Cyrys, J., Heinrich, J., Hoek, G., Meliefste, K., Lewne, M., Gehring, U., Bellander, T., Fischer, P., Van Vliet, P., Brauer, M., Wichmann, H. E., and Brunekreef, B.: Comparison between different traffic-related particle indicators: Elemental carbon (EC), $PM_{2.5}$ mass, and absorbance, J. Expo. Anal. Env. Epid., 13, 134-143, doi:10.1038/sj.jea.7500262, 2003.

Dan, M., Zhuang, G. S., Li, X. X., Tao, H. R., and Zhuang, Y. H.: The characteristics of carbonaceous species and their sources in $PM_{2.5}$ in Beijing, Atmos. Environ., 38, 3443-3452, doi:10.1016/j.atmosenv.2004.02.052, 2004.

Diaz-Robles, L. A., Ortega, J. C., Fu, J. S., Reed, G. D., Chow, J. C., Watson, J. G., and Moncada-Herrera, J. A.: A hybrid ARIMA and artificial neural networks model to forecast particulate matter in urban areas: The case of Temuco, Chile, Atmos. Environ., 42, 8331-8340, doi:10.1016/j.atmosenv.2008.07.020, 2008.

GEPB: Guangzhou Environmental Protection Bureau, available at: http://www.gz.gov.cn/gzgov/s2812/200912/163197.shtml (last assess: 25 May 2017), (in Chinese), 2009.

Guo, J. P., He, J., Liu, H. L., Miao, Y. C., Liu, H., and Zhai, P. M.: Impact of various emission control schemes on air quality using WRF-Chem during APEC China 2014, Atmos. Environ., 140, 311-319, doi:10.1016/j.atmosenv.2016.05.046, 2016.

Han, T. T., Xu, W. Q., Chen, C., Liu, X. G., Wang, Q. Q., Li, J., Zhao, X. J., Du, W., Wang, Z. F., and Sun, Y. L.: Chemical apportionment of aerosol optical properties during the Asia-Pacific Economic Cooperation summit in Beijing, China, J. Geophys. Res., 120, doi:10.1002/2015JD023918, 2015.

Hien, P. D., Bac, V. T., Tham, H. C., Nhan, D. D., and Vinh, L. D.: Influence of meteorological conditions on $PM_{2.5}$ and $PM_{2.5\text{-}10}$ concentrations during the monsoon season in Hanoi, Vietnam, Atmos. Environ., 36, 3473-3484, doi:10.1016/S1352-2310(02)00295-9, 2002.

Huang, X. F., He, L. Y., Hu, M., Canagaratna, M. R., Sun, Y., Zhang, Q., Zhu, T., Xue, L., Zeng, L. W., Liu, X. G., Zhang, Y. H., Jayne, J. T., Ng, N. L., and Worsnop, D. R.: Highly time-resolved chemical characterization of atmospheric submicron particles during 2008 Beijing Olympic Games using an Aerodyne High-Resolution Aerosol Mass Spectrometer, Atmos. Chem. Phys., 10, 8933-8945, doi:10.5194/acp-10-8933-2010, 2010.

715 Kelly, F. J. and Zhu, T.: Transport solutions for cleaner air, Science, 352, 934-936,
716 doi:10.1126/science.aaf3420, 2016.
717 Liu, J., Mauzerall, D. L., Chen, Q., Zhang, Q., Song, Y., Peng, W., Klimont, Z., Qiu, X.
718 H., Zhang, S. Q., Hu, M., Lin, W. L., Smith, K. R., and Zhu, T.: Air pollutant
719 emissions from Chinese households: A major and underappreciated ambient
720 pollution source, P. Natl. Acad. Sci. USA., 113, 7756-7761, doi:
721 10.1073/pnas.1604537113, 2016.
722 Liu, J., and Zhu, T.: NO_x in Chinese Megacities, Nato. Sci. Peace. Secur., 120, 249-263,
723 doi:10.1007/978-94-007-5034-0_20, 2013.
724 Liu, W., Li, X. D., Chen, Z., Zeng, G. M., Leon, T., Liang, J., Huang, G. H., Gao, Z. H.,
725 Jiao, S., He, X. X., and Lai, M. Y.: Land use regression models coupled with
726 meteorology to model spatial and temporal variability of NO_2 and PM_{10} in
727 Changsha, China, Atmos. Environ., 116, 272-280,
728 doi:10.1016/j.atmosenv.2015.06.056, 2015.
729 Liu, Y., Franklin, M., Kahn, R., and Koutrakis, P.: Using aerosol optical thickness to
730 predict ground-level $PM_{2.5}$ concentrations in the St. Louis area: A comparison
731 between MISR and MODIS, Remote. Sens. Environ., 107, 33-44,
732 doi:10.1016/j.rse.2006.05.022, 2007.
733 Liu, Y., He, K. B., Li, S. S., Wang, Z. X., Christiani, D. C., and Koutrakis, P.: A
734 statistical model to evaluate the effectiveness of $PM_{2.5}$ emissions control during
735 the Beijing 2008 Olympic Games, Environ. Int., 44, 100-105,
736 doi:10.1016/j.envint.2012.02.003, 2012.
737 Mukai, H., Tanaka, A., Fujii, T., Zeng, Y. Q., Hong, Y. T., Tang, J., Guo, S., Xue, H. S.,
738 Sun, Z. L., Zhou, J. T., Xue, D. M., Zhao, J., Zhai, G. H., Gu, J. L., and Zhai, P. Y.:
739 Regional characteristics of sulfur and lead isotope ratios in the atmosphere at
740 several Chinese urban sites, Environ. Sci. Technol., 35, 1064-1071,
741 doi:10.1021/es001399u, 2001.
742 Mustaffa, N. I. H., Latif, M. T., Ali, M. M., and Khan, M. F.: Source apportionment of
743 surfactants in marine aerosols at different locations along the Malacca Straits,
744 Environ. Sci. Pollut. R., 21, 6590-6602, doi:10.1007/s11356-014-2562-z, 2014.
745 Nguyen, T. T. N., Bui, H. Q., Pham, H. V., Luu, H. V., Man, C. D., Pham, H. N., Le, H.
746 T., and Nguyen, T. T.: Particulate matter concentration mapping from MODIS
747 satellite data: a Vietnamese case study, Environ. Res. Lett., 10, 095016,
748 doi:10.1088/1748-9326/10/9/095016, 2015.
749 NOAA Air Resources Laboratory: http://ready.arl.noaa.gov/READYamet.php/.
750 Raman, R. S. and Kumar, S.: First measurements of ambient aerosol over an
751 ecologically sensitive zone in Central India: Relationships between $PM_{2.5}$ mass,
752 its optical properties, and meteorology, Sci. Total. Environ., 550, 706-716,
753 doi:10.1016/j.scitotenv.2016.01.092, 2016.

Richmond-Bryant, J., Saganich, C., Bukiewicz, L., and Kalin, R.: Associations of $PM_{2.5}$ and black carbon concentrations with traffic, idling, background pollution, and meteorology during school dismissals, Sci. Total. Environ., 407, 3357-3364, doi:10.1016/j.scitotenv.2009.01.046, 2009.

Schleicher, N., Norra, S., Dietze, V., Yu, Y., Fricker, M., Kaminski, U., Chen, Y., and Cen, K.: The effect of mitigation measures on size distributed mass concentrations of atmospheric particles and black carbon concentrations during the Olympic Summer Games 2008 in Beijing, Sci. Total. Environ., 412, 185-193, doi:10.1016/j.scitotenv.2011.09.084, 2011.

SEPB: Shanghai Environmental Protection Bureau, available at: http://www.sepb.gov.cn/fa/cms/shhj//shhj2272/shhj2159/2010/02/20671.htm (last assess: 25 May 2017), (in Chinese), 2010.

Sotoudeheian, S. and Arhami, M.: Estimating ground-level PM_{10} using satellite remote sensing and ground-based meteorological measurements over Tehran, J. Environ. Health. Sci., 12, 122, doi:10.1186/S40201-014-0122-6, 2014.

Sternbeck, J., Sjodin, A., and Andreasson, K.: Metal emissions from road traffic and the influence of resuspension-results from two tunnel studies, Atmos. Environ., 36, 4735-4744, doi:10.1016/S1352-2310(02)00561-7, 2002.

Takuwa, T., Mkilaha, I. S. N., and Naruse, I.: Mechanisms of fine particulates formation with alkali metal compounds during coal combustion, Fuel, 85, 671-678, doi:10.1016/j.fuel.2005.08.043, 2006.

Tao, J., Gao, J., Zhang, L., Zhang, R., Che, H., Zhang, Z., Lin, Z., Jing, J., Cao, J., and Hsu, S. C.: $PM_{2.5}$ pollution in a megacity of southwest China: source apportionment and implication, Atmos. Chem. Phys., 14, 8679-8699, doi:10.5194/acp-14-8679-2014, 2014.

Tian, J. and Chen, D. M.: A semi-empirical model for predicting hourly ground-level fine particulate matter ($PM_{2.5}$) concentration in southern Ontario from satellite remote sensing and ground-based meteorological measurements, Remote. Sens. Environ., 114, 221-229, doi:10.1016/j.rse.2009.09.011, 2010.

Wang, Z. S., Li, Y. T., Chen, T., Li, L. J., Liu, B. X., Zhang, D. W., Sun, F., Wei, Q., Jiang, L., and Pan, L. B.: Changes in atmospheric composition during the 2014 APEC conference in Beijing, J. Geophys. Res., 120, 12695-12707, doi:10.1002/2015JD023652, 2015.

Wen, W., Cheng, S., Chen, X., Wang, G., Li, S., Wang, X., and Liu, X.: Impact of emission control on PM and the chemical composition change in Beijing-Tianjin-Hebei during the APEC summit 2014, Environ. Sci. Pollut. R., 23, 4509-4521, doi:10.1007/s11356-015-5379-5, 2016.

Wu, Q., Xu, W., and Wang, Z.: The air quality forecast about $PM_{2.5}$ before and during APEC 2014 in Beijing by WRF-CMAQ model system, EGU General Assembly

Conference, 2015.

Yanosky, J. D., Paciorek, C. J., Laden, F., Hart, J. E., Puett, R. C., Liao, D. P., and Suh, H. H.: Spatio-temporal modeling of particulate air pollution in the conterminous United States using geographic and meteorological predictors, Environ. Health., 13, 63, doi:10.1186/1476-069x-13-63, 2014.

You, W., Zang, Z. L., Pan, X. B., Zhang, L. F., and Chen, D.: Estimating $PM_{2.5}$ in Xi'an, China using aerosol optical depth: A comparison between the MODIS and MISR retrieval models, Sci. Total. Environ., 505, 1156-1165, doi:10.1016/j.scitotenv.2014.11.024, 2015.

Zhang, J. P., Zhu, T., Zhang, Q. H., Li, C. C., Shu, H. L., Ying, Y., Dai, Z. P., Wang, X., Liu, X. Y., Liang, A. M., Shen, H. X., and Yi, B. Q.: The impact of circulation patterns on regional transport pathways and air quality over Beijing and its surroundings, Atmos. Chem. Phys., 12, 5031-5053, doi:10.5194/acp-12-5031-2012, 2012.

Zhang, X. Y., Wang, Y. Q., Lin, W. L., Zhang, Y. M., Zhang, X. C., Gong, S., Zhao, P., Yang, Y. Q., Wang, J. Z., Hou, Q., Zhang, X. L., Che, H. Z., Guo, J. P., and Li, Y.: Changes of atmospheric composition and optical properties over Beijing 2008 Olympic monitoring campaign, B. Am. Meteorol. Soc., 90, 1633, doi:10.1175/2009BAMS2804.1, 2009.

Zhang, W., Zhu, T., Yang, W., Bai, Z., Sun, Y. L., Xu, Y., Yin, B., and Zhao, X.: Airborne measurements of gas and particle pollutants during CAREBeijing-2008, Atmos. Chem. Phys., 14, 301-316, doi:10.5194/acp-14-301-2014, 2014.

Atmos. Chem. Phys. Discuss., doi:10.5194/acp-2017-456, 2017
Manuscript under review for journal Atmos. Chem. Phys.
Discussion started: 29 May 2017

Atmospheric Chemistry and Physics Discussions

Figure Captions:

Figure 1. Time series of atmospheric particulate matter of aerodynamic diameter ≤ 2.5 μm ($PM_{2.5}$) and the concentrations of its components, wind direction (WD), wind speed (WS), temperature (T), and relative humidity (RH) before, during, and after (a) APEC 2014 and (b) Parade 2015. The grey-shaded areas highlight the pollution control periods of APEC 2014 (3 November to 12 November 2014) and Parade 2015 (20 August to 3 September 2015).

Figure 2. Proportions of the measured components in $PM_{2.5}$ during (a) APEC 2014 and (b) Parade 2015 campaigns, including organic carbon (OC), elemental carbon (EC), SO_4^{2-}, NO_3^-, NH_4^+, Cl^- and elements. B: before; A: after.

Figure 3. Scatter plot and correlations between organic carbon (OC: *y*-axis) and elemental carbon (EC: *x*-axis) concentrations of $PM_{2.5}$ during the APEC 2014 and Parade 2015 campaigns. The red symbols denote the non-control period and the black symbols denote the pollution control period. The linear regression equations and R^2 values are given for these two campaigns.

Figure 4. Upper panel: time series of the proportion of sulphate, nitrate, and ammonia (SNA) in $PM_{2.5}$ ($\rho(SNA)/PM_{2.5}$) and $PM_{2.5}$ mass concentrations (the black bar represents $PM_{2.5}$ concentration and the red line represents $\rho(SNA)/PM_{2.5}$). Middle panel: SO_2, SO_4^{2-}, and SOR ($[SO_4^{2-}]/([SO_2]+[SO_4^{2-}])$). Lower panel: NO_x, NO_3^-, and NOR ($[NO_3^-]/([NO_x]+[NO_3^-])$). Data collected during the (a) APEC 2014 and (b) Parade

2015 campaigns. The hollow bars represent gaseous pollutants (red for SO_2, blue for NO_x), and solid bars represent secondary inorganic ions (red for sulphate, blue for nitrate).

Figure 5. Wind rose plots based on frequencies of half-hourly data before APEC (BAPEC), during APEC, and after APEC (AAPEC) on the left, and before Parade (BParade), during Parade, and after Parade (AParade) on the right.

Figure 6. Time series of daily $PM_{2.5}$ concentrations and planetary boundary layer (PBL) heights during the (a) APEC and (b) Parade campaigns. The black line represents $PM_{2.5}$ concentrations and the red line represents PBL heights. The grey-shaded areas highlight the pollution control periods of APEC 2014 (3 November to 12 November 2014) and Parade 2015 (20 August to 3 September 2015).

Figure 7. Scatter plot showing the correlation between daily $PM_{2.5}$ concentrations (*y*-axis) and (a) daily PBL heights (*x*-axis) and (b) daily WSs (*x*-axis) during the APEC 2014 sampling period (October to December 2014) and Parade 2015 sampling period (August to December 2015). The red and black scattered points represent different distribution areas. The piecewise function regression equations and the corresponding values of PBL height and WS according to the intersections are given.

Figure 8. The black bars represent the percentage reductions calculated by comparing the decreased average concentrations during APEC to the average concentrations before APEC. The red bars represent the percentage reductions calculated by comparing

863 the decreased average concentrations during APEC to the average concentrations
864 before APEC based only on the days with stable meteorological conditions. The
865 whiskers represent the standard deviations of the percentage reductions.
866
867 Figure 9. Variations of air pollutant concentrations during days with stable
868 meteorological conditions during the APEC 2014 campaign, including $PM_{2.5}$, sulphate,
869 nitrate, and ammonium (SNA), organic carbon (OC), elemental carbon (EC), Cl^-, K^+,
870 elements (Pb, Zn, Ni, Mn, and Ca), and gaseous pollutants (SO_2, NO, NO_x, and O_3).
871 The red points represent mean values. The black cross bars are median values. The
872 black box denotes the 25^{th} and 75^{th} percentiles. The whiskers represent the maximum
873 and minimum, respectively. B: before; A: after.
874
875 Figure 10. Scatter plot and correlations between GLM-predicted (*y*-axis) and observed
876 (*x*-axis) concentrations of pollutants transformed to a natural log. The linear regression
877 equations and R^2 values are given.
878
879 Figure 11. Time series of the observed and cross-validation (CV) predicted $PM_{2.5}$
880 concentrations during five CV periods. The black line represents the observed $PM_{2.5}$
881 concentration and the red line represents the CV-predicted $PM_{2.5}$ concentration.
882
883 Figure 12. Residual analysis of the model. (a) Histogram of the regression standardized
884 residual. (b) Scatter plot between the regression standardized predicted value and
885 regression standardized residual. (c) Normal P-P plot of the regression standardized

Atmos. Chem. Phys. Discuss., doi:10.5194/acp-2017-456, 2017
Manuscript under review for journal Atmos. Chem. Phys.
Discussion started: 29 May 2017

Atmospheric Chemistry and Physics Discussions

residual between the observed cumulative probability and expected cumulative probability. (d) De-trended normal P-P plot of the standardized residual of observed cumulative probability.

Atmos. Chem. Phys. Discuss., doi:10.5194/acp-2017-456, 2017
Manuscript under review for journal Atmos. Chem. Phys.
Discussion started: 29 May 2017

Atmospheric Chemistry and Physics Discussions

891 Table 1. Air pollution control strategies during APEC 2014 and Parade 2015.

Periods	Control measures	Detail of measures
APEC 2014 (3 to 12 November 2014) and **Parade 2015** (20 August to 3 September 2015)	Traffic control	The odd/even plate number rule for traffic control in Beijing, Tianjin, Hebei and Shandong; 70% (APEC 2014)/80% (Parade 2015) of official vehicle and "yellow label vehicles" were banned from Beijing's roads; Trucks limited to run inside the 6th Ring Road between 6 AM to 24 PM.
	Industrial emission control	More than 10,000 factories production limited or halted in Beijing and Hebei, Tianjin, Shandong, Shanxi and Inner Mongolia which surround Beijing city.
	Dust pollution control	Dust emission factories and outdoor constructions shut down or limited in Beijing and near area; Enhancing road cleaning and spray and aspirating in Beijing.
	Coal-fired control	State-owned enterprise productions enhancing limited and 40% coal-fired boilers shut down in Beijing; more special pollutant emission factory limited around Beijing.

892
893

Atmos. Chem. Phys. Discuss., doi:10.5194/acp-2017-456, 2017
Manuscript under review for journal Atmos. Chem. Phys.
Discussion started: 29 May 2017

Atmospheric Chemistry and Physics Discussions

894 Table 2. Summary of statistical models applied to predict air pollutant concentrations
895 with meteorological parameters.

Dependent variables	Independent variables	R^2	Methods*	Applications
$PM_{2.5}$	meteorological parameters (T/RH/PBL/WS/cloud fraction), AOT	0.47	MLR	Gupta and Christopher, 2009
PM_{10}	meteorological parameters (T/WD/RH/PBL/WS), AOD	0.21/0.30 (MODIS/MISR)	MLR	Sotoudeheian and Arhami, 2014
PM_{10}	meteorological parameters (RH/WS/T), AOD	0.49-0.88 (spatial-temporal variability)	MLR	Chitranshi et al., 2015
$PM_{2.5}$	meteorological parameters (T/RH/PREC), AOT	0.60/0.58 (MOD/MYD)	MLR	Nguyen et al., 2015
$\ln(PM_{2.5})$, $\ln(PM_{2.5\text{-}10})$	meteorological parameters (ln(PREC)/ln(RH)/ln(WS)/ln(SUN)/ln(T)), atmospheric turbulence parameters ($\ln(\Delta u/\Delta z)/\ln(\Delta\theta/\Delta z)$)	0.60-0.74	GLM	Hien et al., 2002
$\ln(PM_{2.5})$	meteorological parameters (T/WD/ln(WS)/ln(PBL)), ln(AOT), categorical parameters	0.51/0.62 (MODIS/MISR)	GLM	Liu et al., 2007
$\log(PM_{2.5})$, log(BC)	meteorological parameters (T/wind index), traffic-related parameters	0.62/0.42 ($PM_{2.5}$/BC)	GLM	Richmond-Bryant et al., 2009
$\ln(PM_{2.5})$	meteorological parameters (ln(PBL)/GEO-4 RH/ln(surface RH)/T), ln(AOD)	0.65	GLM	Tian and Chen, 2010
$\ln(PM_{10})$	meteorological parameters (T/WD/RH/ln(PBL)/ln(WS)), ln(AOD)	0.18/0.38 (MODIS/MISR)	GLM	Sotoudeheian and Arhami, 2014
$\ln(PM_{2.5})$	meteorological parameters (ln(PBL)/RH/Vis/ln(T)/ln(WS)), ln(AOD)	0.67/0.72 (MODIS/MISR)	GLM	You et al., 2015
$\ln(PM_{2.5})$	meteorological parameters (WS/WD/T/RH/pressure), optical properties (absorption/scattering/attenuation co-efficient)	0.54/0.31/0.32/0.88 (winter/pre-monsoon/monsoon/post-monsoon)	GLM	Raman and Kumar, 2016
PM_{10}, $PM_{2.5}$	smooth non-parametric functions of spatial/temporal variates	0.58	GAM	Barmpadimos et al., 2012
$PM_{2.5}$, PM_{10}, $PM_{2.5\text{-}10}$	smooth non-parametric functions of spatial/temporal variates	0.77/0.58/0.46-0.52 ($PM_{2.5}$/PM_{10}/$PM_{2.5\text{-}10}$)	GAM	Yanosky et al., 2014
PM_{10}	meteorological parameters ($WS/T_{min}/T_{max}$), previous day PM_{10}	0.78	ANN	Diaz-Robles et al., 2008
$PM_{2.5}$	meteorological parameters (WS/RH/PBL/WS*PBL), AOD, spatial	0.89	LUR	Chudnovsky et al., 2014

	explanatory variables			
PM_{10}, NO_2	meteorological parameters (T/RH/WS/air pressure/cloud cover/percentage of haze/mist/rain/sun), spatial explanatory variables	0.45/0.43 (PM_{10}/NO_2)	LUR	Liu et al., 2015

*MLR: multiple linear regression model, GLM: generalized linear regression model, GAM: generalized additive model, ANN: artificial neural networks, LUR: land use regression model.

896

897

Atmos. Chem. Phys. Discuss., doi:10.5194/acp-2017-456, 2017
Manuscript under review for journal Atmos. Chem. Phys.
Discussion started: 29 May 2017

Atmospheric Chemistry and Physics Discussions

898 Table 3. Meteorological parameters used in the GLM. The calculation of each
899 meteorological parameter is based on the sample duration of 23.5 h (09:30–09:00 LT
900 the next day).

Parameters	Abbreviations	Description
Wind direction value*	WD	The average of wind direction values.
	WD_{sum}	The sum of wind direction values.
	WD_{mode}	The mode of wind direction values.
Wind speed (m s^{-1})	WS	The average of wind speed.
	WS_{mode}	The mode of wind speed.
	WS_{max}	The maximum of wind speed.
Temperature (°C）	T	The average of temperature.
	T_{max}	The maximum of temperature.
	T_{min}	The minimum of temperature.
	ΔT	The difference of temperature.
Sea level pressure (hPa)	SLP	The average of sea level pressure.
	SLP_{max}	The maximum of sea level pressure.
	SLP_{min}	The minimum of sea level pressure.
Relative humidity (%)	RH	The average of relative humidity.
	RH_{max}	The maximum of relative humidity.
Precipitation (mm)	PREC	The accumulation of precipitation.
Wind index	WD/WS	The average of wind direction value/wind speed.
	WD/WS_{sum}	The sum of wind direction value/wind speed.
Planetary boundary layer height (m)	PBL	The average of 3-h planetary boundary layer height.
	PBL_{min}	The minimum of 3-h planetary boundary layer height.
	PBL_{max}	The maximum of 3-h planetary boundary layer height.

* Since the degree data of wind direction cannot be applied directly, the values of wind directions are donated such that value = 1, 2, 3 for north, south, and “calm and variable”, respectively.

901

Atmos. Chem. Phys. Discuss., doi:10.5194/acp-2017-456, 2017
Manuscript under review for journal Atmos. Chem. Phys.
Discussion started: 29 May 2017

Atmospheric Chemistry and Physics Discussions

902 Table 4. Statistical summary showing the mean concentrations and standard deviations
903 of $PM_{2.5}$, gaseous pollutants, and $PM_{2.5}$ components. B: before; A: after.

Pollutants	Units	BAPEC	APEC	AAPEC	BParade	Parade	AParade
$PM_{2.5}$		113±62	48±35	97±84	41±14	15±6	39±28
OC		15.3±8.7	11.2±7.2	21.3±15.5	7.4±1.9	4.0±1.0	6.3±3.1
EC		2.7±1.4	1.7±1.0	3.5±1.8	1.6±0.3	0.8±0.1	2.0±1.0
SO_4^{2-}		12.6±9.1	3.9±3.0	9.6±12.4	10.6±6.2	2.6±1.3	7.9±7.3
NO_3^-		29.4±21.4	10.6±11.0	16.3±19.4	5.0±3.9	1.5±1.5	6.4±6.2
NH_4^+		15.0±10.6	4.8±4.2	10.3±11.9	5.2±2.6	1.5±1.0	5.4±5.4
Cl^-		3.19±1.61	2.06±2.11	6.59±6.67	0.20±0.16	0.16±0.12	0.53±0.24
Na^+	μg m^{-3}	0.50±0.26	0.26±0.15	0.57±0.46	0.16±0.09	0.10±0.05	0.16±0.08
K^+		1.20±0.63	0.65±0.51	1.52±1.43	0.30±0.13	0.18±0.08	0.38±0.20
Mg^{2+}		0.07±0.03	0.09±0.02	0.13±0.07	0.01±0.01	0.01±0.00	0.02±0.01
Ca^{2+}		0.52±0.34	0.28±0.19	0.53±0.40	0.14±0.07	0.10±0.04	0.17±0.05
SO_2		11.3±5.0	9.5±6.8	34.8±15.3	2.7±1.6	1.6±1.4	5.9±5.2
NO		54.2±30.5	21.9±13.8	112.3±63.2	3.2±2.1	1.2±0.9	9.3±7.5
NO_x		151±62	81±46	220±107	57±11	26±13	63±24
O_3		23±16	38±19	17±14	116±33	79±22	74±27
Ca		582±431	591±335	1536±579	202±64	108±36	188±130
Co		0.48±0.21	0.34±0.18	0.90±0.52	0.21±0.08	0.05±0.02	0.16±0.10
Ni		3.20±1.56	5.07±7.42	5.17±2.50	1.75±1.16	0.63±0.72	1.16±0.67
Cu		35.7±16.2	19.1±12.6	43.3±31.2	12.4±5.1	3.7±1.3	9.6±6.5
Zn		320±146	128±120	315±310	97±46	20±9	71±54
Se		6.45±3.46	3.76±3.84	5.22±6.56	7.06±3.41	3.19±2.76	3.17±2.76
Mo		2.20±1.12	1.63±1.14	2.85±2.67	0.62±0.41	0.16±0.14	0.53±0.46
Cd		3.86±2.53	1.41±1.25	3.11±2.52	2.35±5.72	0.22±0.17	0.71±0.74
Tl	ng m^{-3}	1.87±0.90	0.87±1.01	2.03±1.96	0.50±0.31	0.05±0.06	0.33±0.39
Pb		121±59	55±52	104±81	36±19	9±6	29±26
Th		0.09±0.05	0.06±0.03	0.09±0.06	0.02±0.01	0.01±0.01	0.01±0.01
U		0.06±0.02	0.05±0.03	0.09±0.06	0.02±0.01	0.00±0.00	0.01±0.02
Na		529±261	355±209	907±632	182±71	96±39	181±96
Mg		153±94	105±47	236±143	43±13	15±8	24±15
Al		516±324	338±154	588±406	141±82	130±60	136±93
Mn		55.5±23.3	34.5±24.1	61.6±52.4	17.3±6.4	3.6±1.8	14.8±9.2
Fe		755±314	573±336	883±538	269±71	98±28	234±139
Ba		16.3±8.0	11.0±8.4	13.8±8.1	4.7±1.6	1.9±0.6	4.1±2.3

904

905

Atmos. Chem. Phys. Discuss., doi:10.5194/acp-2017-456, 2017
Manuscript under review for journal Atmos. Chem. Phys.
Discussion started: 29 May 2017

Atmospheric Chemistry and Physics Discussions

906 Table 5. Statistical summary showing the meteorological conditions (WS and PBL
907 height), and the concentrations of pollutants on the days with stable meteorological
908 conditions during the APEC campaign. B: before; A: after.

		WS	PBL	$PM_{2.5}$	OC	EC	SO_4^{2-}	NO_3^-	NH_4^+	SO_2	NO	NO_x	O_3
		($m\ s^{-1}$)	(m)	($\mu g\ m^{-3}$)									
	10/18	1.27	145	153	-	-	14.3	43.0	19.4	-	73	240	45.2
	10/22	1.46	233	67	10.9	3.6	7.4	14.0	9.3	12.1	59	153	4.4
	10/23	1.46	188	108	18.0	2.6	11.3	23.7	13.2	11.5	91	200	6.6
	10/24	1.52	171	177	20.5	3.0	24.6	54.2	28.3	12.0	73	205	20.4
BAPEC	10/28	1.71	232	87	15.9	3.8	7.0	17.8	7.9	13.0	69	165	14.2
	10/29	1.10	193	132	23.6	5.3	10.6	35.2	14.0	15.6	99	229	10.0
	10/30	1.00	160	170	26.0	4.0	18.5	56.0	25.7	18.4	77	195	7.5
	10/31	1.50	209	138	17.0	3.9	13.5	29.3	16.1	8.1	79	183	4.6
	Mean	**1.38**	**191**	**129**	**18.8**	**3.7**	**13.4**	**34.2**	**16.7**	**12.9**	**77**	**196**	**14.1**
	11/3	1.98	211	39	11.1	1.8	1.8	4.9	2.6	5.8	19	84	36.5
	11/4	1.85	163	116	22.7	2.9	9.6	33.1	13.2	26.0	31	144	20.5
	11/7	1.63	264	59	12.5	2.8	4.3	10.9	6.1	13.6	30	101	15.0
APEC	11/8	2.00	196	76	17.3	2.4	7.3	21.1	8.8	11.8	26	101	33.6
	11/9	1.79	154	66	17.6	2.5	4.9	14.0	6.3	9.2	44	125	27.7
	11/10	2.13	177	61	14.3	1.8	5.6	17.9	7.5	10.2	31	115	29.2
	Mean	**1.90**	**194**	**70**	**15.9**	**2.4**	**5.6**	**17.0**	**7.4**	**12.7**	**30**	**112**	**27.1**
	11/14	1.58	169	61	15.2	4.5	3.4	6.4	4.1	30.3	87	171	14.7
	11/15	1.38	173	118	24.2	6.6	7.2	19.6	10.6	52.0	148	276	5.0
	11/17	2.48	252	57	14.5	3.8	2.8	4.0	3.7	30.4	125	206	25.0
	11/18	1.44	106	101	27.1	3.8	6.3	14.3	8.3	54.5	162	285	6.2
AAPEC	11/19	1.23	121	267	53.2	5.0	38.2	55.6	35.2	54.6	190	369	1.0
	11/20	1.94	120	220	41.6	3.7	26.2	46.9	28.8	38.8	200	383	2.9
	11/22	1.96	178	58	14.0	3.3	3.3	5.4	4.5	32.2	89	183	26.7
	Mean	**1.72**	**160**	**126**	**27.1**	**4.4**	**12.5**	**21.7**	**13.6**	**41.8**	**143**	**268**	**11.6**

909

Atmos. Chem. Phys. Discuss., doi:10.5194/acp-2017-456, 2017
Manuscript under review for journal Atmos. Chem. Phys.
Discussion started: 29 May 2017

Atmospheric Chemistry and Physics Discussions

910 Table 6. The percentage differences (PD) for the $PM_{2.5}$ concentrations of four periods
911 (P1, P2, P3, and P4) that were randomly selected from within the non-control stable
912 days of the APEC 2014 and Parade 2015 campaigns.

Periods	Mean values ($\mu g\ m^{-3}$)	SD ($\mu g\ m^{-3}$)	Total SD ($\mu g\ m^{-3}$)	Percentage differences (PD)*				Mean PD	RMSE of PD
				P1	P2	P3	P4		
P1	120	97	59	-	-	-	-	-16%	18%
P2	101	58		-16%	-	-	-		
P3	96	40		-20%	-5%	-	-		
P4	87	23		-28%	-14%	-9%	-		

* Percentage difference (PD) = (Mean value of P_{n+1} - Mean value of P_n)/Mean value of $P_n \times 100\%$.

913
914

Atmos. Chem. Phys. Discuss., doi:10.5194/acp-2017-456, 2017
Manuscript under review for journal Atmos. Chem. Phys.
Discussion started: 29 May 2017

Atmospheric Chemistry and Physics Discussions

915 Table 7. The cross-validation (CV) performance of the $PM_{2.5}$ GLM.

Periods	Adjusted R^2	Observed mean values (μg m^{-3})	Predicted mean values (μg m^{-3})	Daily RMSE (μg m^{-3})	Total RMSE (μg m^{-3})	Relative errors (RE)*	Mean RE	RMSE of RE
CV1	0.748	94	82	53		15%		
CV2	0.798	59	57	20		4%		
CV3	0.783	44	52	19	33	-15%	-5%	14.6%
CV4	0.710	54	65	27		-17%		
CV5	0.807	41	47	30		-13%		

*Relative error (RE) = (Predicted mean value - Observed mean value)/Predicted mean value × 100%.

916

Atmos. Chem. Phys. Discuss., doi:10.5194/acp-2017-456, 2017
Manuscript under review for journal Atmos. Chem. Phys.
Discussion started: 29 May 2017

Atmospheric Chemistry and Physics Discussions

Table 8. The concentrations of air pollutants for the GLM with adjusted R^2 values higher than 0.6.

Pollutants	Model descriptions	Adjusted R^2
$PM_{2.5}$	$\ln(PM_{2.5})$=-0.48lnWS-0.43$\ln WS_{max(lag)}$-0.00076PBL_{max}-0.11PREC+0.25ln$\Delta T_{(lag)}$-0.14WS_{mode}+0.48WD/$WS_{(lag)}$+0.0043$PBL_{min(lag)}$-0.025$PREC_{(lag)}$-0.015SLP_{min}+19.51	0.808
EC	ln(EC)=0.60lnWD/WS_{sum}-0.59lnPBL-0.017$PREC_{(lag)}$+0.22lnΔT-0.50ln$WS_{(lag)}$+0.25ln$PBL_{max(lag)}$-0.17	0.780
OC	ln(OC)= -0.44lnWS+0.47WD/$WS_{(lag)}$-0.67lnPBL-0.020$PREC_{(lag)}$+0.67lnWD+0.17lnΔT-0.65ln$RH_{max(lag)}$+7.84	0.751
SO_4^{2-}	ln(SO_4^{2-})=-0.99ln$WS_{(lag)}$+0.066T_{min}-0.040$PREC_{(lag)}$-1.20lnPBL+0.0011$PBL_{(lag)}$+0.019RH-0.12PREC+0.087WS_{max}+6.68	0.795
NO_3^-	ln(NO_3^-)=-1.90lnPBL-0.96ln$WS_{(lag)}$+0.88WD+0.0045PBL_{min}-0.20PREC+0.12WS_{max}+1.57lnRH+0.60ln$\Delta T_{(lag)}$-1.22ln$RH_{max(lag)}$-0.047ΔT+9.32	0.833
NH_4^+	ln(NH_4^+)=0.040RH-1.27ln$WS_{(lag)}$-1.03ln$RH_{(lag)}$-0.00075PBL_{max}-0.16PREC+0.33ln$\Delta T_{(lag)}$+4.28	0.813
Cl^-	ln(Cl^-)= -1.12lnPBL-0.072$T_{(lag)}$+1.60lnWD-2.32ln$RH_{max(lag)}$+0.53lnWD/$WS_{sum(lag)}$+14.69	0.737
K^+	ln(K^+)= -0.75lnPBL-0.66ln$WS_{(lag)}$-0.020$RH_{(lag)}$+0.0056PBL_{min}-0.20WS_{mode}+0.33ln$\triangle T_{(lag)}$-0.47ln$PBL_{max(lag)}$-0.087PREC+0.66lnRH+5.46	0.717
Pb	ln(Pb)= -0.61lnWS-0.67ln$WS_{max(lag)}$+0.36ln$\Delta T_{(lag)}$-0.00062PBL_{max}-0.19WS_{mode}-0.030$PREC_{(lag)}$+5.39	0.721
Zn	ln(Zn)=-0.81lnWS-0.41ln$WS_{max(lag)}$-0.0016PBL-0.36ln$WS_{mode(lag)}$+6.56	0.627
Mn	ln(Mn)=0.80WD/WS-0.98lnPBL-0.043$PREC_{(lag)}$+0.57WD/$WS_{(lag)}$-0.017RH-0.023SLP+0.0030$PBL_{min(lag)}$+31.04	0.656
SO_2	ln(SO_2)=-1.32lnPBL-0.071$PREC_{(lag)}$-0.047PREC+0.29$WD_{mode(lag)}$-0.026RH-0.47ln$WS_{(lag)}$+14.12lnSLP_{max}-87.56	0.803
NO_x	ln(NO_x)=0.014WD/WS_{sum}-0.030T_{min}+0.27lnΔT-0.44lnPBL-0.015PREC-0.012$PREC_{(lag)}$+5.30	0.772

Atmos. Chem. Phys. Discuss., doi:10.5194/acp-2017-456, 2017
Manuscript under review for journal Atmos. Chem. Phys.
Discussion started: 29 May 2017

Atmospheric Chemistry and Physics Discussions

Table 9. The output indexes of the $PM_{2.5}$ GLM, including a model summary, analysis of variance (ANOVA), coefficients, and other indexes.

Model Summary and ANOVA						
R	R^2	Adjusted R^2	Std. Error of the Estimate	Durbin-Watson	F	Sig.*
0.910	0.828	0.808	0.411	1.910	41.763	0.000

Coefficients						
Model	Unstandardized Coefficients		t	Sig.*	Collinearity Statistics	
	B	Std. Error			Tolerance	VIF
(Constant)	19.512	6.871	2.840	0.006		
lnWS	-0.483	0.162	-2.971	0.004	0.313	3.194
$lnWS_{max(lag)}$	-0.431	0.153	-2.818	0.006	0.300	3.331
PBL_{max}	-0.001	0.000	-6.747	0.000	0.395	2.534
PREC	-0.110	0.029	-3.735	0.000	0.618	1.618
$ln\triangle T_{(lag)}$	0.247	0.083	2.975	0.004	0.662	1.512
WS_{mode}	-0.135	0.050	-2.726	0.008	0.493	2.027
$WD/WS_{(lag)}$	0.476	0.148	3.222	0.002	0.353	2.829
$PBL_{min(lag)}$	0.004	0.001	3.510	0.001	0.407	2.459
$PREC_{(lag)}$	-0.025	0.009	-2.796	0.006	0.707	1.415
SLP_{min}	-0.015	0.007	-2.176	0.032	0.707	1.414

*The significance level is 0.05.

Atmos. Chem. Phys. Discuss., doi:10.5194/acp-2017-456, 2017
Manuscript under review for journal Atmos. Chem. Phys.
Discussion started: 29 May 2017

Atmospheric Chemistry and Physics Discussions

923 Table 10. The percentage differences between the observed and GLM-predicted
924 concentrations of the air pollutants during APEC and Parade.

Pollutants	Units	During APEC			During Parade		
		Observed	Predicted	Percentage differences[1]	Observed	Predicted	Percentage differences[1]
$PM_{2.5}$	μg m^{-3}	48	67	28%	15	20	25%
OC		11.2	12.6	11%	4.0	3.7	-8%
EC		1.7	2.7	37%	0.8	1.2	33%
SO_4^{2-}		3.9	2.7	-44%	2.6	5.2	50%
NO_3^-		10.6	19.0	44%	1.5	3.4	56%
NH_4^+		4.8	5.5	13%	1.5	2.4	38%
Cl^-		2.06	2.58	20%	0.16	0.17	6%
K^+		0.65	1.03	37%	0.18	0.24	25%
Pb	ng m^{-3}	55	70	21%	9	17	47%
Zn		128	171	25%	20	41	51%
Mn		34.5	51.5	33%	3.6	7.6	53%
SO_2	ppb	3.32	6.59	50%	0.57	0.56	-2%
NO_x		45	102	56%	13	20	35%
OC+EC	μg m^{-3}	12.9	15.3	16%	4.8	4.9	2%
SNA	μg m^{-3}	19.3	27.2	29%	5.6	11.0	49%
total S[2]	μmol m^{-3}	0.189	0.322	41%	0.053	0.079	33%

[1]Percentage difference = (Predicted - Observed)/Predicted × 100%.

[2]total S = $[SO_2]$ + $[SO_4^{2-}]$.

925

926

Atmos. Chem. Phys. Discuss., doi:10.5194/acp-2017-456, 2017
Manuscript under review for journal Atmos. Chem. Phys.
Discussion started: 29 May 2017

Atmospheric Chemistry and Physics Discussions

927

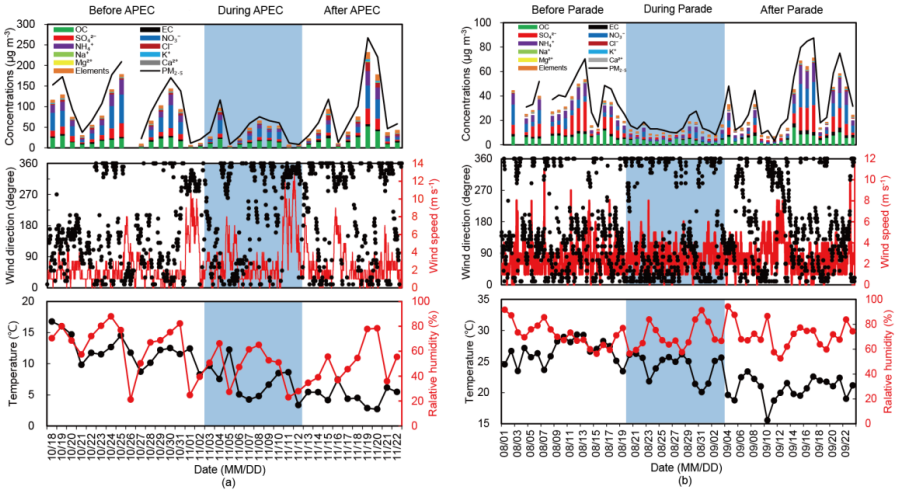

928

929 Figure 1. Time series of atmospheric particulate matter of aerodynamic diameter ≤ 2.5
930 μm ($PM_{2.5}$) and the concentrations of its components, wind direction (WD), wind speed
931 (WS), temperature (T), and relative humidity (RH) before, during, and after (a) APEC
932 2014 and (b) Parade 2015. The grey-shaded areas highlight the pollution control periods
933 of APEC 2014 (3 November to 12 November 2014) and Parade 2015 (20 August to 3
934 September 2015).

935

Atmos. Chem. Phys. Discuss., doi:10.5194/acp-2017-456, 2017
Manuscript under review for journal Atmos. Chem. Phys.
Discussion started: 29 May 2017

Atmospheric Chemistry and Physics Discussions

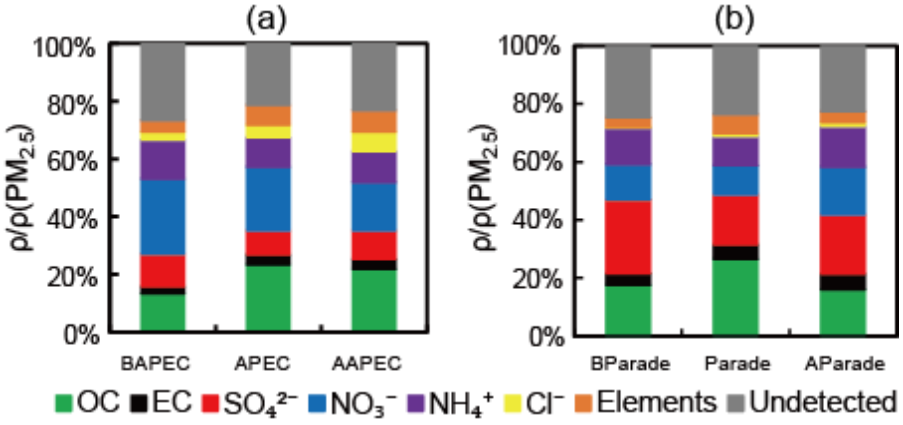

936

937 Figure 2. Proportions of the measured components in $PM_{2.5}$ during (a) APEC 2014 and

938 (b) Parade 2015 campaigns, including organic carbon (OC), elemental carbon (EC),

939 SO_4^{2-}, NO_3^-, NH_4^+, Cl^- and elements. B: before; A: after.

940

Atmos. Chem. Phys. Discuss., doi:10.5194/acp-2017-456, 2017
Manuscript under review for journal Atmos. Chem. Phys.
Discussion started: 29 May 2017

Atmospheric Chemistry and Physics Discussions

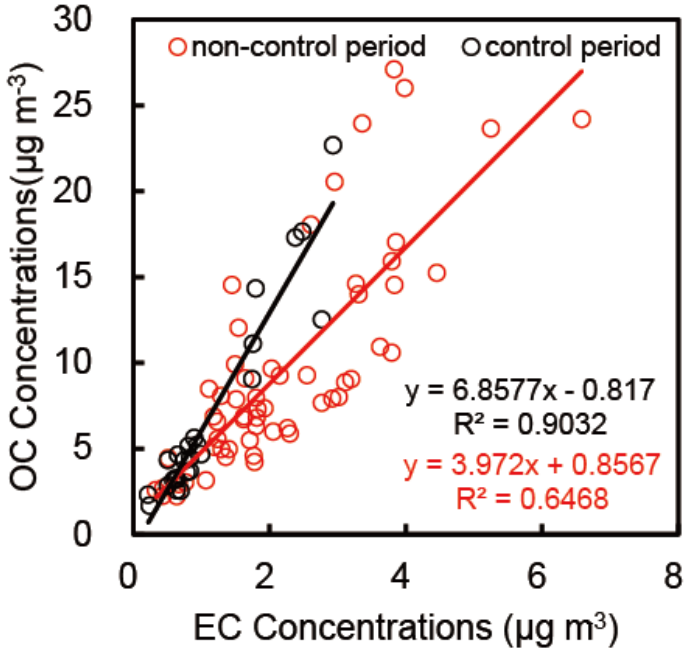

941

942 Figure 3. Scatter plot and correlations between organic carbon (OC: *y*-axis) and
943 elemental carbon (EC: *x*-axis) concentrations of $PM_{2.5}$ during the APEC 2014 and
944 Parade 2015 campaigns. The red symbols denote the non-control period and the black
945 symbols denote the pollution control period. The linear regression equations and R^2
946 values are given for these two campaigns.

947

Atmos. Chem. Phys. Discuss., doi:10.5194/acp-2017-456, 2017
Manuscript under review for journal Atmos. Chem. Phys.
Discussion started: 29 May 2017

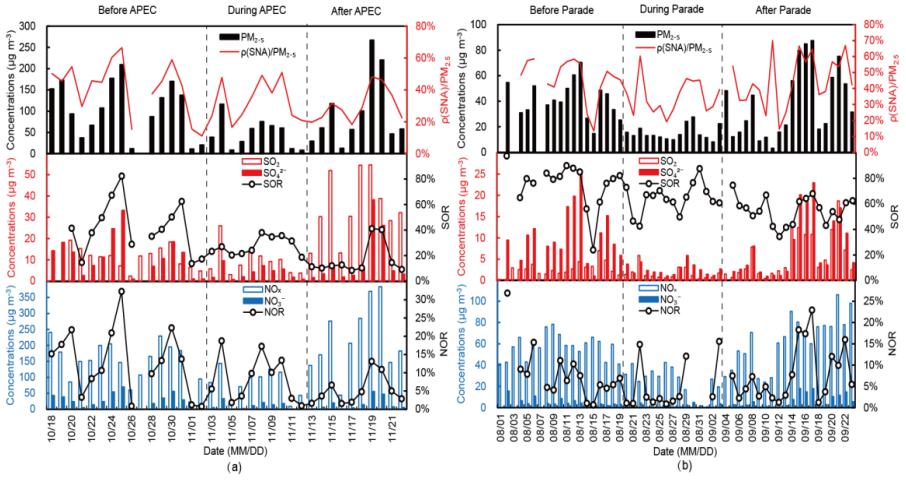

Figure 4. Upper panel: time series of the proportion of sulphate, nitrate, and ammonia (SNA) in $PM_{2.5}$ ($\rho(SNA)/PM_{2.5}$) and $PM_{2.5}$ mass concentrations (the black bar represents $PM_{2.5}$ concentration and the red line represents $\rho(SNA)/PM_{2.5}$). Middle panel: SO_2, SO_4^{2-}, and SOR ($[SO_4^{2-}]/([SO_2]+[SO_4^{2-}])$). Lower panel: NO_x, NO_3^-, and NOR ($[NO_3^-]/([NO_x]+[NO_3^-])$). Data collected during the (a) APEC 2014 and (b) Parade 2015 campaigns. The hollow bars represent gaseous pollutants (red for SO_2, blue for NO_x), and solid bars represent secondary inorganic ions (red for sulphate, blue for nitrate).

Atmos. Chem. Phys. Discuss., doi:10.5194/acp-2017-456, 2017
Manuscript under review for journal Atmos. Chem. Phys.
Discussion started: 29 May 2017

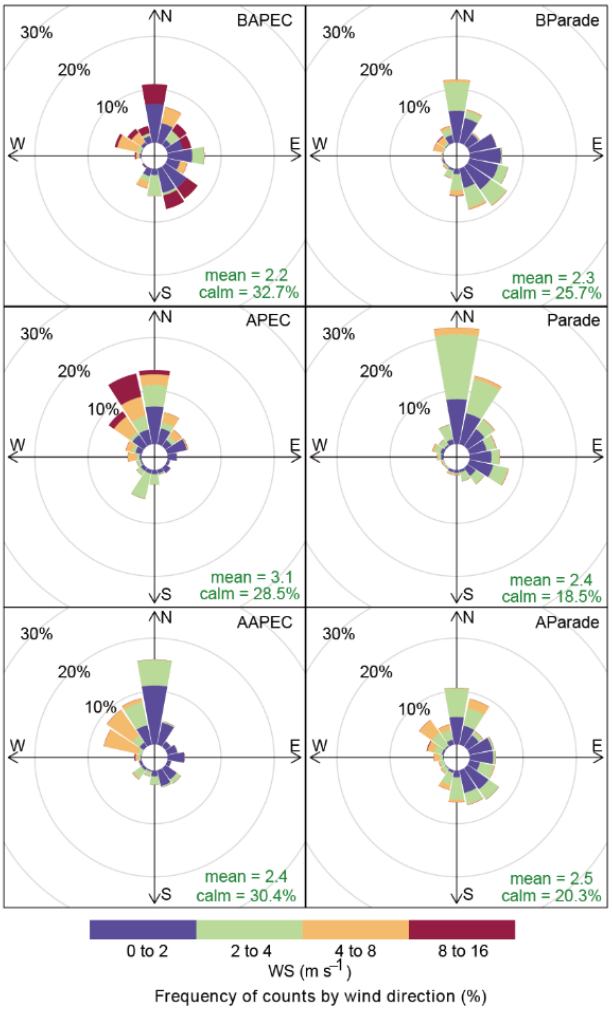

Figure 5. Wind rose plots based on frequencies of half-hourly data before APEC (BAPEC), during APEC, and after APEC (AAPEC) on the left, and before Parade (BParade), during Parade, and after Parade (AParade) on the right.

Atmos. Chem. Phys. Discuss., doi:10.5194/acp-2017-456, 2017
Manuscript under review for journal Atmos. Chem. Phys.
Discussion started: 29 May 2017

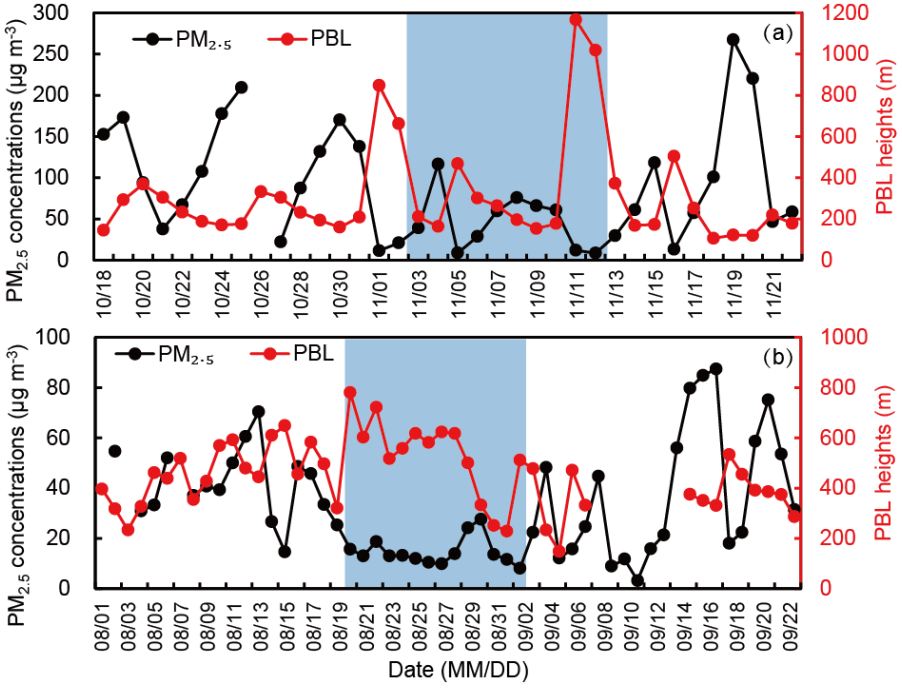

963

964 Figure 6. Time series of daily $PM_{2.5}$ concentrations and planetary boundary layer (PBL)

965 heights during the (a) APEC and (b) Parade campaigns. The black line represents $PM_{2.5}$

966 concentrations and the red line represents PBL heights. The grey-shaded areas highlight

967 the pollution control periods of APEC 2014 (3 November to 12 November 2014) and

968 Parade 2015 (20 August to 3 September 2015).

969

Atmos. Chem. Phys. Discuss., doi:10.5194/acp-2017-456, 2017
Manuscript under review for journal Atmos. Chem. Phys.
Discussion started: 29 May 2017

Atmospheric Chemistry and Physics Discussions

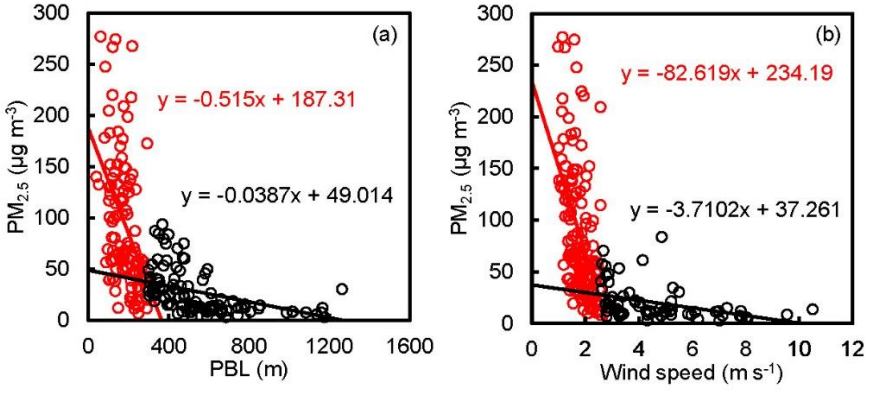

Values of intersections

PBL (m)	Wind speed (m s^{-1})
290	2.50

Figure 7. Scatter plot showing the correlation between daily $PM_{2.5}$ concentrations (*y*-axis) and (a) daily PBL heights (*x*-axis) and (b) daily WSs (*x*-axis) during the APEC 2014 sampling period (October to December 2014) and Parade 2015 sampling period (August to December 2015). The red and black scattered points represent different distribution areas. The piecewise function regression equations and the corresponding values of PBL height and WS according to the intersections are given.

Atmos. Chem. Phys. Discuss., doi:10.5194/acp-2017-456, 2017
Manuscript under review for journal Atmos. Chem. Phys.
Discussion started: 29 May 2017

Atmospheric Chemistry and Physics Discussions

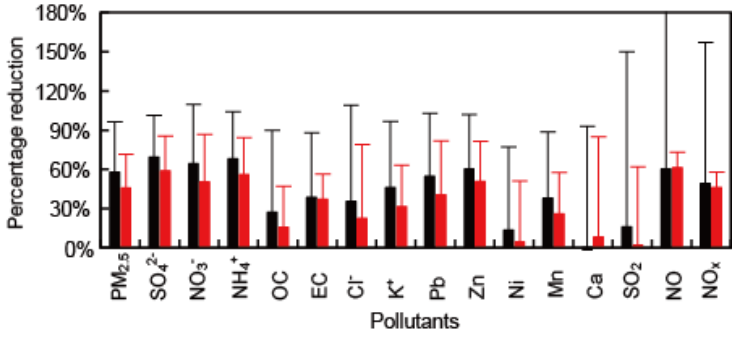

978

979 Figure 8. The black bars represent the percentage reductions calculated by comparing
980 the decreased average concentrations during APEC to the average concentrations
981 before APEC. The red bars represent the percentage reductions calculated by comparing
982 the decreased average concentrations during APEC to the average concentrations
983 before APEC based only on the days with stable meteorological conditions. The
984 whiskers represent the standard deviations of the percentage reductions.

Atmos. Chem. Phys. Discuss., doi:10.5194/acp-2017-456, 2017
Manuscript under review for journal Atmos. Chem. Phys.
Discussion started: 29 May 2017

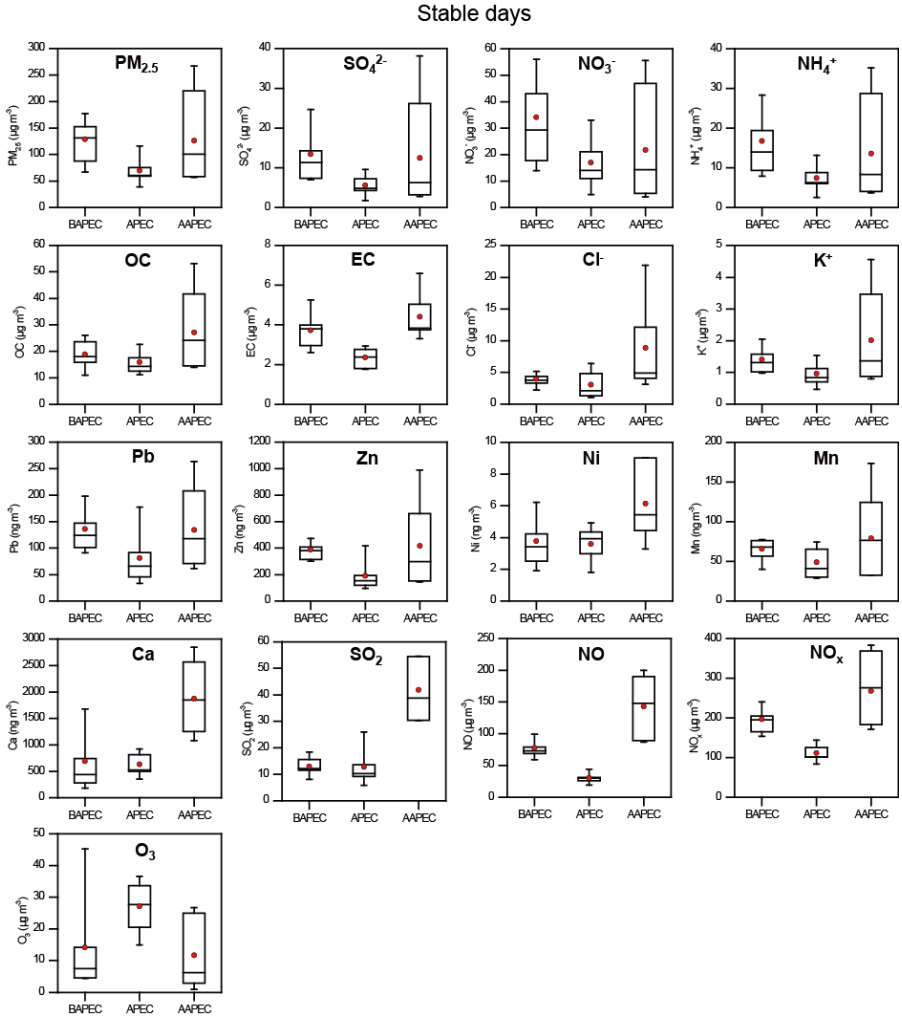

Figure 9. Variations of air pollutant concentrations during days with stable meteorological conditions during the APEC 2014 campaign, including $PM_{2.5}$, sulphate, nitrate, and ammonium (SNA), organic carbon (OC), elemental carbon (EC), Cl^-, K^+, elements (Pb, Zn, Ni, Mn, and Ca), and gaseous pollutants (SO_2, NO, NO_x, and O_3). The red points represent mean values. The black cross bars are median values. The black box denotes the 25th and 75th percentiles. The whiskers represent the maximum and minimum, respectively. B: before; A: after.

Atmos. Chem. Phys. Discuss., doi:10.5194/acp-2017-456, 2017
Manuscript under review for journal Atmos. Chem. Phys.
Discussion started: 29 May 2017

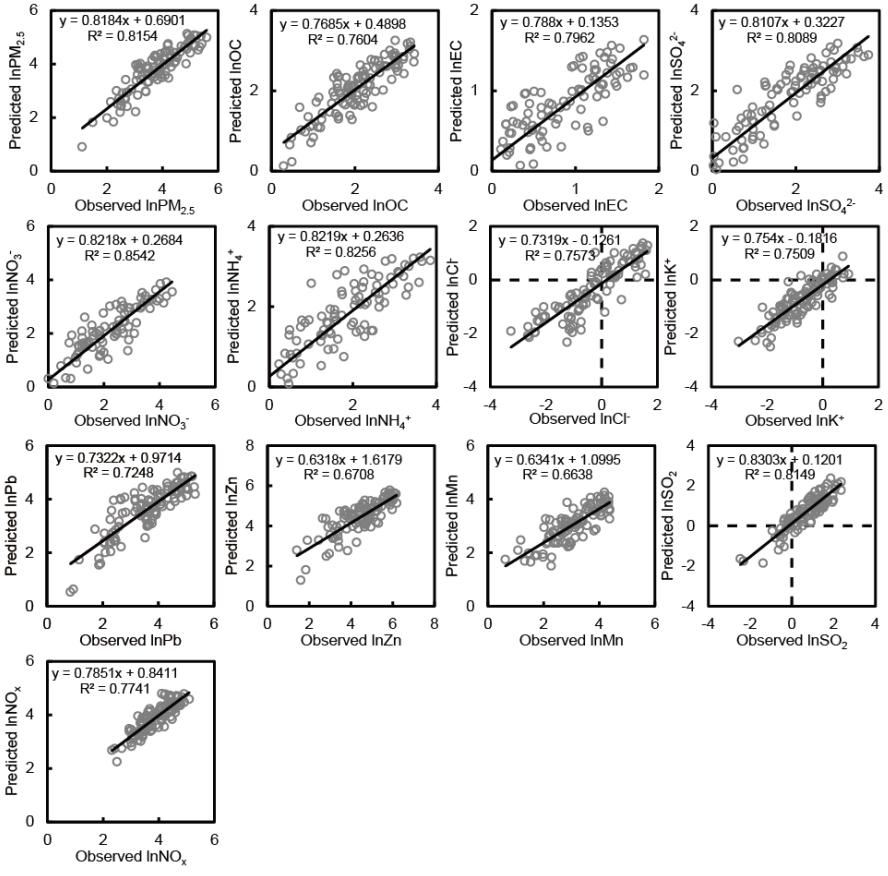

Figure 10. Scatter plot and correlations between GLM-predicted (*y*-axis) and observed (*x*-axis) concentrations of pollutants transformed to a natural log. The linear regression equations and R^2 values are given.

Atmos. Chem. Phys. Discuss., doi:10.5194/acp-2017-456, 2017
Manuscript under review for journal Atmos. Chem. Phys.
Discussion started: 29 May 2017

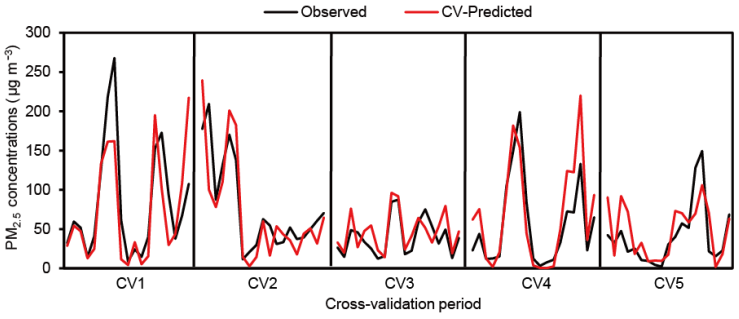

1000

1001 Figure 11. Time series of the observed and cross-validation (CV) predicted $PM_{2.5}$

1002 concentrations during five CV periods. The black line represents the observed $PM_{2.5}$

1003 concentration and the red line represents the CV-predicted $PM_{2.5}$ concentration.

1004

Atmos. Chem. Phys. Discuss., doi:10.5194/acp-2017-456, 2017
Manuscript under review for journal Atmos. Chem. Phys.
Discussion started: 29 May 2017

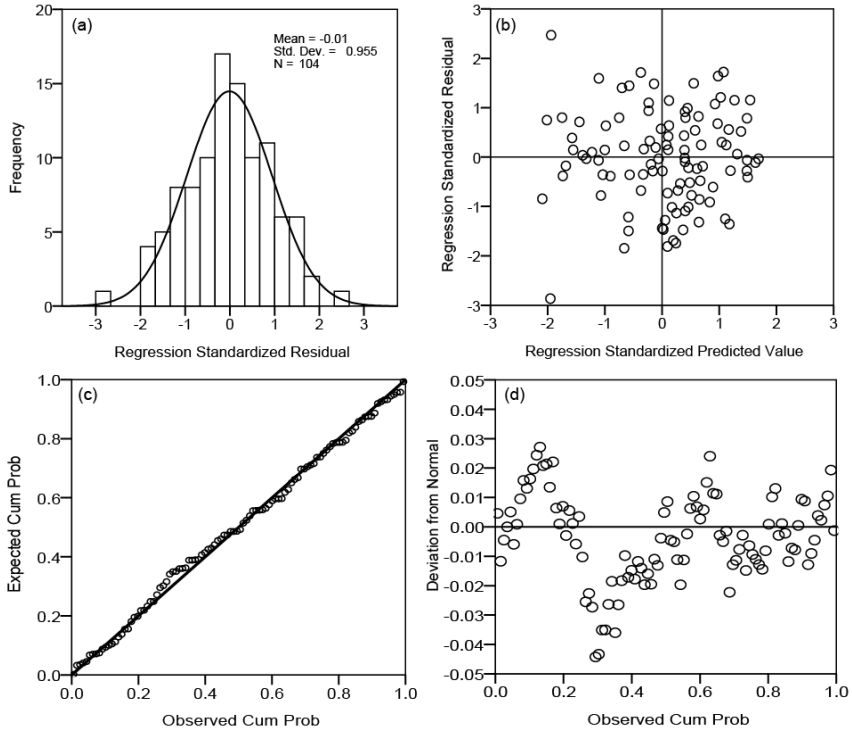

Figure 12. Residual analysis of the model. (a) Histogram of the regression standardized residual. (b) Scatter plot between the regression standardized predicted value and regression standardized residual. (c) Normal P-P plot of the regression standardized residual between the observed cumulative probability and expected cumulative probability. (d) De-trended normal P-P plot of the standardized residual of observed cumulative probability.